Yale Medicine Thesis Digital Library   School of Medicine

January 2018

Retinal Stem Cell Culture On Planar Scaffold For Transplantation In Animal Models Of Retinal Degeneration

Tina Xia

Follow this and additional works at: https://elischolar.library.yale.edu/ymtdl

Retinal stem cell culture on planar scaffold for transplantation

in animal models of retinal degeneration

A Thesis Submitted to the
Yale University School of Medicine
in Partial Fulfillment of the Requirements for the
Degree of Doctor of Medicine

By

Tina Xia

2018

ABSTRACT

RETINAL STEM CELL CULTURE ON PLANAR SCAFFOLD FOR
TRANSPLANTATION IN ANIMAL MODELS OF RETINAL DEGENERATION

Tina Xia, Deepti Singh, Shaobin Wang, Scott Ketner, Ron Adelman, Lawrence Rizzolo.
Department of Ophthalmology and Department of Surgery-gross anatomy, Yale
University School of Medicine, New Haven, CT.

Successful differentiation of pluripotent stem cells into retinal cells and subsequent

transplantation in animal models have made stem cell-based therapy a closer possibility for

treating retinal degenerations. However, major limitations are low efficiency in deriving

desired cell types and continued need for large animal studies to validate small animal

studies. In this study, we modified a biopolymer scaffold with laminin-521 as a novel

substrate to culture retinal progenitor cells (RPCs). We hypothesize that laminin-521 will

increase cell retention and provide a developmental signal for RPCs to mature and self-

organize. The RPC scaffold culture was transplanted into a RD10 mice, a rodent model of

retinal degeneration to evaluate the effects on disease pathology, and into pig eyes for a

large animal pilot transplantation study. Differentiation of RPC was monitored by qRT-

PCR, immunofluorescence and immunoblotting. Graft survival, integration, and host

immune reactivity was assessed via histology and immunofluorescence. The laminin-521

coated scaffold (GCH-L521) increased cell attachment compared to non-coated scaffold.

GCH-L521 was able to support growth and continued differentiation of RPC. When

transplanted into animal models, the RPC scaffold graft survived in the host and did not

cause significant host immune reaction. In RD10 mice, transplantation resulted in

improved photoreceptor preservation. GCH-L521 can serve as a new substrate to culture

RPC and simultaneously functions as a transplantation vehicle that is well-tolerated in the

host.

1

ACKNOWLEDGEMENT

The project would not be possible without the contributions and guidance of my mentors, colleagues and collaborators. I would like to thank Dr. Lawrence Rizzolo and Dr. Ron Adelman for the wonderful mentorship during my research year and for the support in helping me develop my career.

To my lab mates, I am grateful for the generous help along the way. I want to acknowledge Deepti Singh, for contributing her expertise on biomaterials and scaffold synthesis. I am grateful for her enthusiastic help with the scaffold cultures and the pig transplantation project, and above all, I am grateful for her encouragement and friendship. To Shao-bin Wang, for sharing his knowledge of molecular biology and for helping with the mice transplantation experiments. To Tao Xu, for being a great companion and problem solver in lab.

I would like to acknowledge Dr. Ron Adelman and Dr. Scott Ketner for their generous time in carrying out the pig transplantation surgeries.

I want to thank Yale School of Medicine Office of Student Research for providing the research support and funding to complete my thesis project. This thesis was supported by grants from NIH Institute on Aging, Connecticut Stem Cell Research, and the Department of Defense.

Lastly, I want to thank my friends for the wonderful memories through our medical school years and my research year. Also to my family, for the unconditional love and support along the way.

TABLE OF CONTENTS

TABLE OF FIGURES

LIST OF ABBREVIATIONS

Age related macular degeneration	AMD
Central nervous system	CNS
Embryoid body	EB
Gelatin-chondroitin sulfate-hyaluronic acid	GCH
Human embryonic stem cells	hESC
Induced pluripotent stem cells	iPSC
Internal limiting membrane	ILM
Laminin 521	L521
Multifocal electroretinogram	mfERG
Optical coherence tomography	OCT
Retinal cup	RC
Retinal pigment epithelium	RPE
Retinal progenitor cell	RPC
Retinitis pigmentosa	RP
Vascular endothelial growth factor	VEGF

INTRODUCTION

Pluripotent stem cells, such as embryonic stem cells (ESC) and induced pluripotent stem cells (iPSC), are promising tools for regenerative medicine and transplantation. There is growing research on stem cell therapy in neurodegenerative diseases, including Alzheimer's, amyotrophic lateral sclerosis, and retinal degeneration [2-4]. Retinal tissue has been differentiated successfully from stem cells and demonstrated positive efficacy results when transplanted into rodent models. However, efficient cell cultures that produce transplantable tissue with long-term treatment efficacy remain a challenge.

The Retina and Retinal Degeneration

The retina is the neurosensory tissue that lines the inside of the eye; it processes and conveys light signals to the brain. An integral part of the retina is the retinal pigment epithelium (RPE), which forms the outer brain-retinal barrier and regulates ion and nutrition balance and waste removal from the retina [5]. The retina contains intricately connected layers of specialized neurons, all functioning to transduce electrical signal from the photoreceptors to the ganglion cells and to the CNS (Figure 1).

Retinal degeneration describes the death of retinal cells from a variety of causes, leading to vision loss and reduced functionality for the patients. Two common forms of retinal degeneration are retinitis pigmentosa (RP) and age-related macular degeneration (AMD). RP is a heterogeneous disease caused by a number of genetic mutations affecting photoreceptor function, leading to degeneration [6]. The etiology of AMD is complex and likely a combination of genetic and environmental factors, and its pathology is thought to begin with degeneration of either the RPE or the photoreceptors [7]. Additionally, AMD is currently the leading cause of blindness in the elderly population of developed countries,

with 2 million people affected in the United States [8]. With the aging population, the prevalence in the US is projected to increase two-fold by 2020. From a public health perspective, this will be a significant increase in the burden of disease.
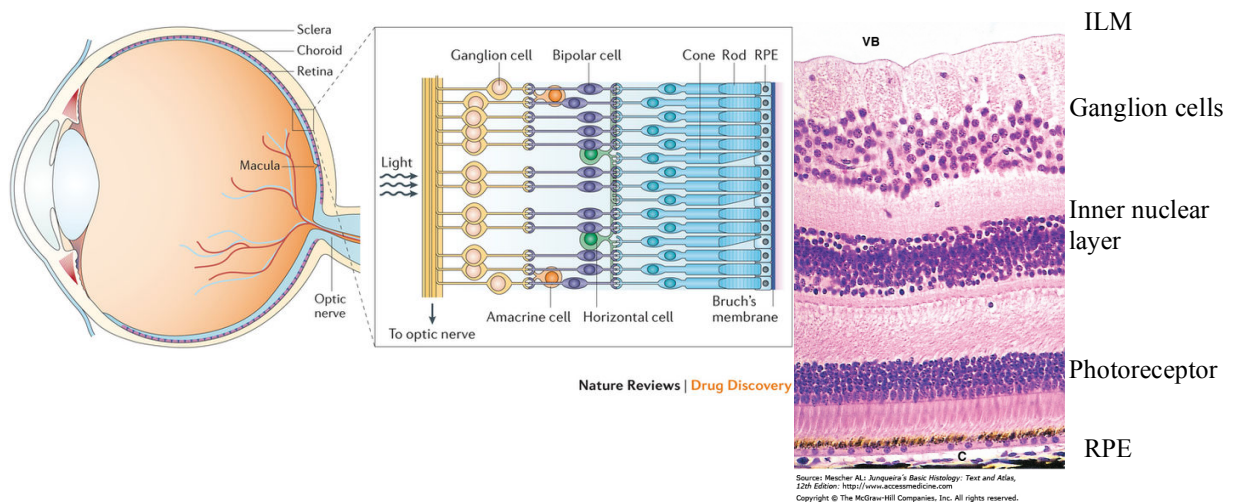
Figure 1. Eye anatomy and retinal layers. Histology of retina. Schematic diagram copied with permission from Kimbrel and Lanza, 2015 [1]. Histology photo adapted from *Junqueira's Basic Histology: Text and Atlas, 12th Edition*.

Currently, treatments of AMD work to prevent progression of disease or to address the signs and complications of disease. In early stages of AMD, AREDS vitamins consisting of vitamin E, vitamin C, copper, zinc, lutein, and zeaxanthin, can be taken to retard progression to advanced disease characterized by abnormal neovascularization, but the efficacy is low [9]. The mainstay of treatment for advanced AMD involve laser procedures and intraocular anti-VEGF injections to prevent worsening pathology. For RP, there is currently no widespread, effective therapy. However, active research is looking into neuroprotective drugs, gene therapy and vision prosthesis for the disease [6]. Stem cell therapy is also under active investigation for AMD, RP and other retinal disease; this modality is aimed at replacing the deteriorating tissue of the retina to regain visual function.

Stem Cells Therapy for Retinal Diseases

Stem cells have therapeutic potential due to their pluripotency state. Pluripotent cells can self-renew and differentiate into many different types of tissue; therefore, stem cells are a potential source of unlimited tissue for research and treatment. The embryonic stem cell (ESC) and induced pluripotent stem cell (iPSC) are pluripotent cells most commonly used to generate differentiated tissue. iPSCs are adult cells that have been reprogrammed back to a pluripotent state through the introduction of four transcription factors Oct3/4, Sox2, Klf4, and c-Myc, a method first described by Dr. Yamanaka in 2006 [10, 11]. Many types of specialized tissue cells are able to be differentiated from pluripotent stem cells, including retinal cells, pancreatic islet cells, hepatocytes, and neural progenitor cells, to name a few [12-14]. In order for stem cells to be therapeutic, the differentiated tissue must resemble native tissue in structure and function, and can survive and contribute to function within the host.

Retinal cells have been successfully differentiated from stem cells. RPE derived from ESC and iPSC exhibited similar pigmentation, morphology and gene expression as primary human fetal RPE [15-17]. With the appropriate culture conditions, stem cell-derived RPE also developed the expected RPE functions, such as maintaining transepithelial resistance (TER) as an epithelium and phagocytosis of photoreceptor outer segments for waste removal [17-19]. Because RPE consists of one cell type, it is easier to differentiate to yield consistent, uniform cultures compared to differentiating the neural retina which contains many different types of retinal neurons. In part, due to this reason, stem-cell derived RPE has been more extensively studied than retinal progenitor cells (RPCs), with more data from both animal studies and patient clinical trials.

However, in many retinal diseases including advanced AMD, the neural retina becomes damaged. Transplanting new RPE may better support the host retina but it ultimately does not replace the degenerating photoreceptors and other retinal neurons. To address this challenge, RPCs also have been differentiated from stem cells with the goal of recapitulating retinal development to produce the different neural retinal cells. Notably, 3D retinal organoids that resemble optic vesicles in early eye organogenesis have been cultured from stem cells using several approaches [20-24]. With time, these retinal organoids develop into retinal cups (RC) and acquired laminations containing cells that express markers for differentiating photoreceptor, amacrine, horizontal and ganglion cells. One group supported RC cultures for 27 weeks and demonstrated the formation of photoreceptor outer segment, a morphologic feature characteristic of photoreceptors and indicated maturation of these neurosensory cells [25]. A small number of these photoreceptors even exhibited electrical signal in response to a light stimulus measured via patch clamp; this encouraging result suggested some degree of functional maturation as well.

The long culture times and an ongoing need to generate mature functional retinal cells from RPCs remain major challenges to translating stem cell-derived retinal cups into treatments for patients. Many improvements have been made in the differentiation protocols for deriving RPE and RPC from stem cells. For example, RPE cultures can be enriched by supplementing ESCs with nicotinamide and activin A and Wnt and Nodal antagonists [19, 21, 26]. The substrates on which retinal cells attach and grow also play a critical role in the maturation process in culture. It has been shown that growing RPE cells on a porous mesh surface, such as poly(l-lactide-co-ε-caprolactone) and parylene-C coated

with extracellular matrix, resulted in more functionally and morphologically mature cells [27-29]. These studies demonstrated the importance of understanding the cellular niche conditions for growing and differentiating retinal cells. There is concurrent research in substrates and matrices that can facilitate maturation of RPC.

Scaffolds and Laminin Proteins in Retinal Culture

Early studies transplanting retinal cups containing RPCs or purified photoreceptor precursors in rodent models yielded promising results for cell engraftment with some functional improvement. However, the limitations were the low efficiency of cell survival and integration in the host retina [30, 31]. An additional limitation of using retinal cups for transplantation is the spherical shape of the organoids, which prevented the RPCs from laying as a flat sheet when implanted underneath the host retina. Investigators attempted to overcome this latter limitation by cutting retinal cups in half to decrease the degree of curvature [32]. However, control of retinal cup orientation was still challenging, as some cells reformed its more spherical shape.

Three-dimensional scaffolds are being studied as a substrate for culturing RPC and as a vehicle for transplantation. Planar scaffolds can aid RPCs to grow in an organized flat conformation, which is easier to insert for subretinal transplantations. Additionally, scaffolds can support more RPC cells because they provide ample surface area for more cells to attach and proliferate [33, 34]. Some studies have shown that the mechanical properties of the scaffolds, such as stiffness and surface topography, can improve retinal differentiation. For example, polycaprolactone (PCL) scaffold etched with linear ridges and grooves promoted RPC proliferation and subsequent photoreceptor differentiation [35].

Previous work from Dr. Lawrence Rizzolo's lab synthesized and characterized a novel 3-D scaffold for culturing RPC. The scaffold has a porous structure due to the lyophilization process and is composed of gelatin, chondroitin-sulfate, and hyaluronic acid, termed the GCH scaffold (Figure 2A). Larger scaffold blocks were sectioned into 60µm thick discs and RPCs were seeded onto the scaffold (Figure 2B). Previous results showed that GCH scaffold supported faster RPC differentiation from human ESC [36]. Additionally, RPC cultured on GCH had greater expression of markers for various differentiating neurons within the retina compared to RPC cultured on 2-D commercially available culture substrate. This project aimed to investigate a further modification of the GCH scaffold to improve the efficiency of RPC cultures. Laminin-521, an extracellular protein, was used to coat GCH scaffold before culturing RPCs.

To promote cell attachment in cultures, scaffolds can be coated with extracellular matrix proteins such as collagen, fibronectin and laminin. Laminin proteins are found abundantly in the extracellular matrix of tissues. Laminins have a heterotrimeric structure comprised of an α chain, a β chain, and a γ chain, with each chain type having several isoforms. In addition to increasing cell attachment, laminins play important roles in directing polarized cell migration and retinal cellular function during the early development of the distinct retinal layers [37, 38]. Disruption of β2 chain, for example, can lead to abnormal photoreceptor morphology and loss synaptic formation [39].

The laminin-521 used in this project is composed of α5, β2, and γ1 chains. We chose to coat the GCH scaffold with laminin-521 because and is the most abundant laminin in the internal limiting membrane (ILM) [40]. The ILM functions as a basement membrane separating the inner retina from the vitreous (Figure 1). As a basement membrane, it

provides a platform for cell attachment and cell compartmentalization. But the ILM also may function to maintain retinal polarity and ganglion cell organization. When the ILM is interrupted, there is significant loss of adjacent ganglion cells, disorganization of the ganglion cell layer, as well as retraction of neuron processes [41, 42]. These studies suggest that the ILM has a role in retinal cell differentiation and survival. Laminin-521 may be a crucial extracellular protein of the ILM in directing cell attachment and retinal polarity.
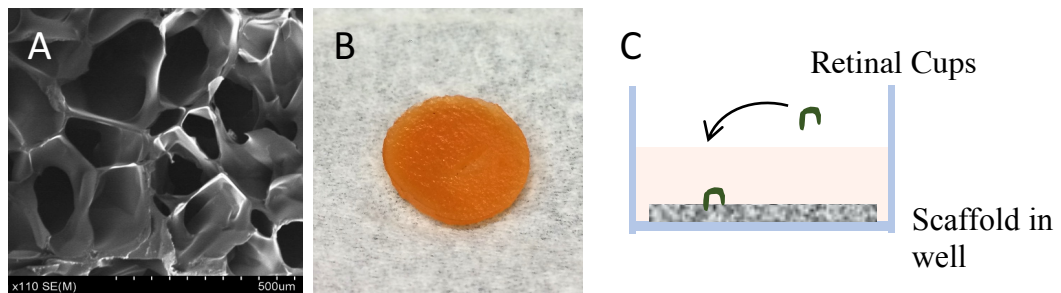
Figure 2. GCH scaffold and culture model. A) scan electron microscopy of scaffold; image provided by Dr. Deepti Singh. B) thicker section of scaffold, to be sectioned into 60µm thickness C) RC containing RPC are seeded onto GCH scaffold in media.

Retinal Transplantation Studies

A major goal of tissue engineering is to obtain a transplantable graft capable of replacing diseased tissue. Transplantation of stem cell-derived RPE and RPC have been studied in animal models, and clinical trials in humans are ongoing. Early transplantation studies were carried out in animal models of retinal degeneration such as the Royal College of Surgeon (RCS) rats, which has a mutation in MERTK and models retinitis pigmentosa [43]. ESC and iPSC-derived RPE transplanted in these rodent models resulted in less photoreceptor degeneration when compared to non-transplanted eyes [43-46]. Transplanted eyes also exhibited better visual function when measured with electroretinogram (ERG) or

optokinetic testing [45, 46]. These results highlighted the potential efficacy of RPE transplantation, but the challenges were how to maintain survival of transplanted cells and the functional improvement for the long-term.

In addition to RPE, transplantation of stem cell-derived RPC into animal models have also been investigated and demonstrated integration of RPCs with the host retina. RPCs migrated into the retinal layers and some cells formed synaptic connections with host retinal cells [31, 32, 47, 48]. On functional testing, transplanted eyes performed better than control eyes. As previously discussed, the culture conditions, such as substrates and trophic supplements, can affect the differentiation of RPC in significant ways. Qu et al. found that the length of time RPCs are cultured in suspension before being seeded onto a flat surface influenced whether the RPCs contained more retinal glial cells or neuronal cells [47]. When left in suspension culture longer, RPCs contained more neuronal cells and when transplanted in RCS rats resulted in better ERG signals than animals transplanted with RPCs that were differentiated for a shorter period of time in suspension. Ongoing research continues to investigate these nuances of the culture microenvironment in order to improve differentiation methods and achieve more mature and functional RPCs.

Despite the challenges of translating stem cell therapy to humans, RPE transplantation are being studied in patients. A phase I/II study transplanted human ESC-derived RPE in patients with AMD and patients with Stargardt's macular dystrophy. The results demonstrated safety and tolerability of the procedure as a primary endpoint [49, 50]. Visual acuity was measured as a secondary endpoint. After six months, four out of the nine AMD patients and three out of the eight Stargardt's patient demonstrated improvement in

visual acuity of 15 letters or more. Although patients on average scored higher on a subjective quality-of-life after their transplantation, the improvement in vision was modest.

Most recently, retinal transplantation using autologous iPSC-derived RPE was performed for the first time in a single patient. The patient's skin fibroblasts were converted to iPSCs and then differentiated into RPE. Like the study mentioned above, the primary aim of the iPSC-RPE study was to demonstrate safety of the iPSC-derived cells [51]. The grafts were well-tolerated with no abnormal growth at the transplant site. Additionally, the patient's vision neither improved nor decreased; however, without a comparison to the control eye, it is difficult to interpret this visual stability.

The next challenge in retinal transplantation clinical trials is to move beyond proof-of-concept studies and demonstrate meaningful improvement in vision. To use research resources effectively, more preclinical work is still needed to explore ways of improving the efficacy of retinal transplantations. Large animal studies can play a role in filling this gap of knowledge. Pigs share many characteristics with the human eye; they have similar sizes and retinal vasculature. Physiologically, the electroretinogram signals are similar between pig and human eyes, and pig eyes contain a region (the visual streak) analogous to the human macula, where vision is the most acute [52-54]. Previous studies in the pig showed survival of transplanted RPC and RPE, with RPCs exhibiting some degree of integration with the host retina [55-58]. RPCs were able to mature further after transplantation in the pig retina [58, 59]. In addition, scaffolds were also tested as vehicles for transplantation in the pig [55, 59]. However, no large animal studies have studied stem-cell derived RPCs in a 3-D scaffold model. This project also aimed to test the laminin-521 coated GCH scaffolds in the pig. Further studies in large animals not only will allow

refinement of transplantation techniques, they can also provide further insight into the physiology of the retina.

Statement of Purpose

Degenerative retinal disorders are debilitating diseases, for which there are no current effective treatments to reverse and restore vision. Stem cell based therapies are a possibility for restoring visual function, and both animal studies and clinical trial yielded promising results. However, the ongoing challenges are to improve the efficacy and consistency in differentiation methods and to derive tissue that can significantly restore function. The purpose of this work is to evaluate the modification of the GCH scaffold with laminin-521 by assessing its ability to support RPC proliferation and differentiation. This project also transplanted the RPC scaffold model in two animal models, mice and pigs, to assess the biocompatibility of the scaffold and to evaluate for any therapeutic effects.

Aims

1. **To increase cell attachment and improve RPC differentiation by culturing on laminin-521 coated GCH (GCH-L521) scaffolds**

   We hypothesized that laminin-521 coating will results in great numbers of RPC cell attachment and retention on the scaffold compared to non-coated scaffolds. Additionally, because laminin-521 is a prominent component of the ILM, the laminin coated scaffold may provide a differentiation signal and promote further maturation and polarization of neural retinal cells.

2. **To ameliorate retinal degeneration in RD10 mice, a model of RP, by transplanting RPC GCH-L521 scaffold grafts**

We hypothesize that the transplanted RPC scaffold graft will slow the degeneration of photoreceptors in the transplanted eye. Disease pathology will be assessed on histology and immunofluorescence. Functional recovery will be assessed with multifocal ERG.

3. **To assess tolerability of scaffold culture graft in pig eyes and optimize post-surgical immunosuppression protocol.**

We hypothesize that the approved surgical procedure and post-operative immunosuppression protocol will be sufficient to control post-operative inflammation and any immune reaction to the scaffold xenograft. Adverse effects of the procedure will be assessed with daily monitoring. Histology and immunofluorescence will be used to assess immune reaction at the tissue level. Dosage of prednisone steroids will be increased if significant amount of inflammatory reactivity is observed.

METHODS

GCH scaffold synthesis and laminin coating

The planar scaffold was fabricated via a freeze dry process from gelatin (500mg), chondroitin sulfate (250mg), and hyaluronic acid (500mg) (GCH) dissolved in 10mL of distilled water [36]. Briefly, gelatin, chondroitin sulfate, and hyaluronic acid were dissolved in distilled water. The polymers were then crosslinked by adding reagents glutaraldehyde. The crosslinked solution was transferred into 3cc syringes to yield a cylindrical shape, frozen for 18hrs at -20°C, and then vacuum dried with a lyophilizer. To obtain thin circular scaffold disks, the cylindrical GCH monolith was frozen in OCT, and sectioned with cryotome with 60μm thickness.

I sterilize scaffolds for cell culture by incubating scaffolds in 70% ethanol overnight. Then scaffolds were washed with PBS three times, then incubated in PBS with 10% penicillin-streptomycin for 30 min before incubating overnight in NIM. For laminin coating, GCH scaffolds were placed into individual wells in a 12-well pate without media. Laminin-521 is gently pipetted onto the scaffold for even coating, and then incubated at 37°C for 30 min.

Differentiation of retinal progenitor cells(RPC)- done by Tina Xia

WA09 human embryonic stem cells were obtained from the Yale Stem Cell Center. WA09 cells were cultured on plates coated with 1% Matrigel and in mTeSR-1 media. Media was changed every 1-2 days and spontaneously differentiating cells were removed under a sterile microscope.

For RPC differentiation, a previously established protocol was used [20]. WA09 cells are incubated with 1U/mL dispase for 30min at 37°C, then blebbstatin is added to the culture. The cells are then cultured in low-attachment, Lipidure-COAT Plates (Amsbio, Abingdon, UK) to induce embryoid body (EB) formation. On initial day of differentiation (D0), EBs were incubated in mTeSR-1. On D1, the EBs were switched to neural induction media (NIM) in 1:3 dilution with mTeSR-1. The NIM contained Dulbecco's modified Eagle's medium (DMEM) with high glucose, F-12 nutrient medium, 15% knockout serum, 1% N2 supplement, 0.1mM 2-mercaptoethanol, 0.1M nonessential amino acids, 1mM glutamax, 50U/mL penicillin, and 50µg/mL streptomycin. On D2, EBs were incubated in NIM was mixed with mTeSR-1 in 1:1 dilution. From days 3 onward, EBs were incubated with only NIM. At D21, spherical retinal cups containing retinal progenitor cells were dissected away from the rest of the EB and seeded on GCH scaffolds. NIM was changed 3 times per week.

To assess cell attachment efficiency, ten EBs were seeded onto each sterilized scaffold, with or without laminin-521 coating. The number of EBs still attached to laminin-521 coated or non-coated scaffolds was counted at 48hrs after seeding.

Scaffold degradation assay

Laminin-521 coated and non-coated scaffolds were incubated in PBS at 37°C with solution change every 3 days. Each week, the scaffold was removed from solution, dried on absorbent paper and weighed. Scaffolds were tested in triplicates. The data is presented as percentage of originate weight:

$$\left(\frac{Weight_x}{Weight_i}\right) \times 100$$

x -weight at certain week

i -initial weight

Quantitative real-time RT-PCR

Cellular RNA was extracted using the TRIzol reagent (Qiagen). RPC on GCH scaffold were sonicated in TRIzol briefly to dissociate the cells and the scaffold before extraction. 1μg of total RNA was used for cDNA synthesis, using iScript Advanced cDNA synthesis kit (Bio-Rad). iTaqSYBR Green (Bio-Rad) was used for the real-time PCR reaction. Primer oligos were synthesized at the Keck Biotechnology Resource Laboratory. All samples were done in triplicates. Relative gene expression was normalized to GAPDH, and calculated using $2^{-\Delta\Delta Ct}$.

Immunoblot

Protein was extracted from WA09 cells or RPCs on scaffold by incubating in lysis buffer with protease inhibitor, 25mM Tris-HCl and 2% SDS. Samples were vortexed and sonicated to ensure adequate extraction from RPC in the scaffolds, then incubated at room temperature for 10 min. Samples were then centrifuged for 10 min at 4°C. Equal amount of protein were loaded into and ran in a 4-20% gradient PAGE gel according to manufacturer protocol. After transfer on to nitrocellulose paper, the blot was washed with TBST, blocked with 5% milk, and incubated with primary antibody overnight in 4°C. Then, the blot was washed again with TBST and incubated with secondary antibody according to manufacturer protocol. Chemiluminescent reagents were added to the bot and imaged with the ChemiDoc system (Bio-Rad).

Immunofluorescence and confocal microscopy

RPC cultures on scaffold were fixed with 4% paraformaldehyde (PFA) for 5min, washed with PBS, and incubated sequentially in 10% and 30% sucrose for 1 hour each. Then RPC scaffolds were incubated overnight in 1:1 solution of OCT and 30% sucrose at 4°C. Then RPC scaffolds were embedded in OCT and cross sectioned with cryotome to 12μm sections mounted on poly-lysine coated slides. Slides were allowed to dry for 48hrs before storing in -20°C. For staining, slides were washed 3 times with PBS and permeabilized for 1hr at room temperature with 0.30% Triton-X100 in PBS. After washing with PBS, slides were blocked with 10% donkey serum and 0.10% Triton-X100 in PBS for 1hr. Samples were then incubated overnight at 4°C with primary antibodies in blocking solution, according to manufacturer recommendations on concentration. After washing with PBS, samples were incubated with secondary chromophore antibodies plus DAPI for 1 hr. After final PBS wash, slides were mounted for imaging.

For preparing pig tissue slides, fresh harvested eyes were incubated in 4% PFA for 1hr, then the cornea and iris is removed circumferentially and vitreous is carefully removed with gentle pipetting. The dissected eye is put back in 4% PFA for an additional 1-2 hrs at 4°C. Then eyes are transferred to 10% sucrose for 6hrs, and then to 30% sucrose overnight in 4°C. Before sectioning, eyes are incubated in a 1:1 mixture of OCT and 30% sucrose for 1 hr. Then, tissue is mounted in OCT, sectioned at 12μm thickness, and mounted on poly-lysine coated slides.

The migration of RPC on scaffold, with or without laminin-521, was assessed by DAPI staining to visualize the migration of cell nuclei. RPC differentiation was monitored by staining for retinal development markers PAX6, RAX, LHX2, CHX10, OTX2, CRX,

recoverin, BRN3, NEUROD1. For pig samples, TRA-1-85 stain was used to identify transplanted cells; IL-6 and IBA-1 were used to assess for inflammation and microglia activation, respectively, from transplantation. An LSM 410 spinning-disc confocal microscope was used to image the samples.

Histology and hematoxylin and eosin staining

Mice and pig eye tissue was collected, cryopreserved and sectioned onto poly-lysine coated slides as described above. Slides were stained with hematoxylin and eosin for tissue structure analysis. Images were captured using the OptraSCAN digital pathology scanner.

RD10 mouse transplantation

Mice experiments were in compliance with and approved by the Yale University Institutional Animal Care and Use Committee (IACUC). For scaffold transplantation, D21 RPC on GCH scaffold were transplanted subretinally in RD10 mice. On postnatal day 30 (P30), RD10 mice were adequately anesthetized by intraperitoneal injection of ketamine at 100mg/kg. Using small surgical scissors, a small incision is made in the lateral conjunctiva and sclera of one eye and 1μL of PBS was injected between the choroid and retina to create a small retinal detachment. A 0.5cm x 0.5cm piece of scaffold with RPC was inserted in the potential space using forceps. RD10 mice were kept in a dark environment for 1-2 days after transplantation, then returned to routine animal facility maintenance. Eyes were harvested at 6 to 10 weeks post-transplantation for tissue analysis.

Pig optical coherence tomography (OCT) and multi-focal electroretinogram (mfERG)-

OCT was acquired while animals were under anesthesia either before surgical procedure or before euthanasia. Two drops of phenylephrine 2.5% and tropicamide 1% each were applied to the test eye for dilation. A Cirrus HD-OCT 4000 (Zeiss) was used to capture the OCT, using the Macula Cube 512x128 scan pattern. Animals were positioned up to the lens, and OCT was scanned when images of good signal can be detected.

For the mfERG, measurements were taken before surgery procedures or before euthanasia. The surgery or control eye of sedated animals were dilated as described above. A RETImap machine (Roland Consult, Germany) was used to capture the mfERG. The test animal was covered with a field shielding blanket to reduce electrical noise artifacts during measurement. In addition, all unnecessary electronics were shut down during mfERG recordings. 2.5% hypromellose eye lubricant was applied on a contact lens ERG electrode and placed on the cornea. Two reference electrodes were placed in the skin of the animal's scalp and front leg. The animal, machine, and shielding blanket were grounded. mfERG measurements were captured according to manufacturer's protocols. A minimum of 10 cycles were ran per recording to obtain reliable mfERG waveforms.

Pig retinal transplantation

Pig experiments were carried out in compliance with Yale University IACUC regulations and with approved protocols. Yorkshire breed pigs were used for all transplantation experiments. Animals were sedated by Yale veterinarian services. 0.2mg/kg of atropine was given intramuscularly at the time of sedation by veterinarians. Additional drops of phenylephrine 2.5% and tropicamide 1% were applied to surgical eye. The eye and

surrounding skin was cleaned with 10% providone-iodine solution and then surgically draped. A 23G pars plana vitrectomy was done to remove the vitreous. Sterile saline solution was injected subretinally using a 38G cannula to create a bleb. The retinal incision site on the bleb was cauterized with diathermy to prevent bleeding. A retinotomy was made using microscissors along the cauterized retina. The scaffold was placed flatly in the subretinal space using a specialized inserter device. Fluid-air exchange (FAX) was done to flatten the transplant site, and air was left in the globe to tamponade the retina. Scleral incision sites were sutured if needed to prevent gas leakage from the eye. At the completion of surgery, 1mg of triamcinolone was injected intravitreally and 50mg of cefazolin was injected under the conjunctiva. (Surgery done by Dr. Ron Adelman and Dr. Scott Ketner, assisted by Tina Xia)

Animals given a buprenorphine patch for the three days post-operatively and systemic steroids (prednisone 2mg/kg) every day until end of experiment. Animals were monitored daily for ocular and systemic symptoms.

Statistical Analysis

Statistical analysis was done using unpaired t-test and one-way ANOVA. Standard error of measurement (SEM) is indicated in the data figures.

RESULTS

Laminin-521 was coated onto pre-fabricated gelatin-chondroitin sulfate-hyaluronic acid (GCH) scaffolds via electrostatic bonding. Therefore, GCH-L521 scaffolds retained the same porous structure as non-coated GCH scaffolds. To assess whether laminin-521 affected the structural integrity of the polymer scaffold, a simple degradation assay was done which showed less degradation of the laminin-521 coated scaffold by week 1 and week 2 compared to non-coated scaffolds. By week 3, there was no significant difference between the two types of scaffolds (Fig 3). It is noted that there was greater variability in the weight measurements at three weeks, which may explain the non-significance observed at that time point.
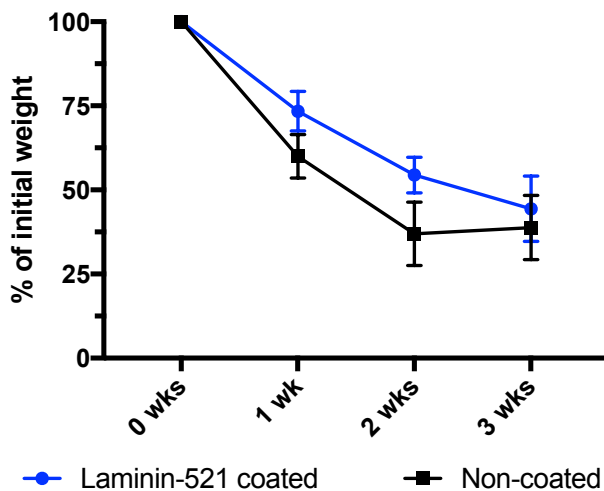
Figure 3. GCH scaffold degradation assay. Wet weight was measured and normalized to initial scaffold weight. Experiments done in triplicates, repeated twice.

Laminin-521 coated GCH scaffold promoted higher cell attachment and migration on scaffold.

Laminin-521 is the predominant laminin protein found in the ILM, and is thought to play a role in embryonic retinal development [40, 60]. Therefore, we hypothesize that laminin-521 modification of the GCH scaffold may facilitate cell migration into the scaffold matrix.

24

As an initial experiment, embryoid bodies (EBs) were seeded onto laminin-521 coated (GCH-L521) and non-coated scaffolds (GCH) and the percentage of EB attachment after 48 hours was calculated. About 25% more EB cell clusters were attached to laminin-coated scaffolds compared to non-coated ones (Fig 4A). Cell migration was assessed by imaging cell nuclei within the scaffold thickness. When retinal cups containing RPCs were seeded onto GCH-L521, the RPCs populated the pores of the scaffold and migrated through its entire thickness (Fig 4B, C).
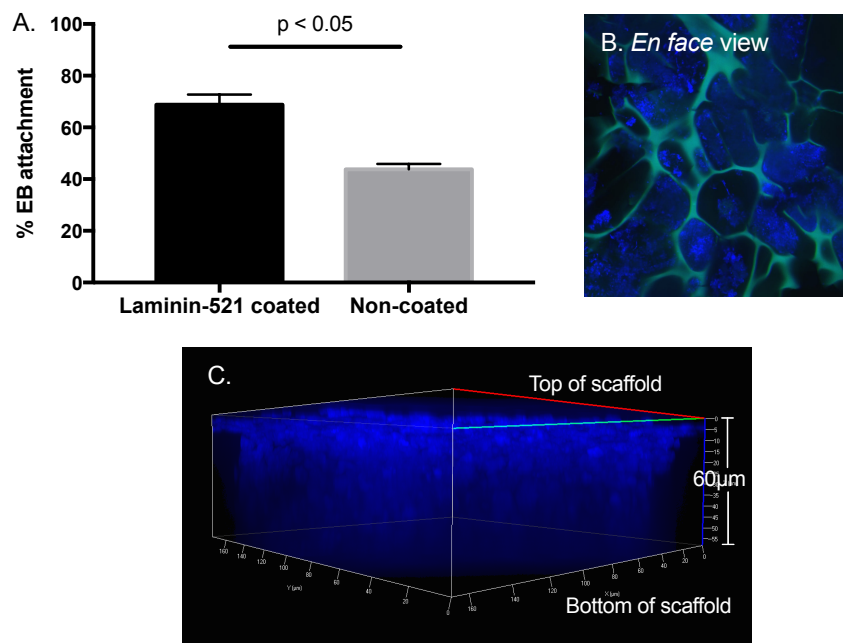
Figure 4. A) Cell attachment on GCH-L521 scaffold 48 hours after seeding. ± SEM. B) *En face* view of RPCs in scaffold. DAPI stains cell nuclei. C) Cross sectional image of RPC nuclei in GCH-L521. Scaffold thickness is 60μm.

**Laminin-521 GCH scaffold supported the differentiation of RPC**

Although cells were able to attach and migrate on the GCH-L521 scaffold, it is essential that the scaffold also supports continued differentiation of RPC into the different types of retinal cells. Nine days after seeding on scaffold (total day 30 of differentiation), RPC continued to express early retinal markers RAX, PAX6, and LHX2. LHX2 is a homeobox

transcription factor that helps to initiate retinal development from the anterior neural plate and later mediates Müller cell gliogenesis [61, 62]. RAX is a homeobox gene also involved in directing early retinal differentiation and retinal stem cell proliferation [63]. PAX6 is an important master regulator that is actively expressed in RPCs during differentiation [64]. In the D30 cultures, RPC on laminin-521 coated scaffolds expressed LHX2 and PAX6 at significantly higher levels than RPC on non-coated scaffolds (Figure 5A). Ki67 is a marker for actively proliferating cells. Although Ki67 expression in both laminin-coated and non-coated cultures decreased compared to early D3 cells, RPC on GCH-L521 had higher Ki67 expression than on non-coated scaffolds, indicating possibly higher cell proliferation on laminin-coated scaffolds (Figure 5A). By D42 (three weeks after seeding onto scaffold), retinal differentiation between laminin-coated and non-coated cultures are comparable, with similar expression of RAX, BRN3 and SIX6. RPC on non-coated GCH scaffolds expressed higher levels of PAX6, LHX2 and NEUROD1 by D42 (Figure 5B). At this later time in differentiation, markers of retinal cell specification began to be expressed. NEUROD1, for example, is a transcription activator that mediates retinal ganglion cell and amacrine cell differentiation[65], and BRN3 is active in ganglion cell differentiation[66].

Expression of NANOG and OCT4 were monitored to ensure differentiation away from the pluripotency state. Interestingly, by D30, the expression of NANOG and OCT4 were increased compared to early baseline expression (D3) in both scaffold cultures, most notably being OCT4 levels. However, by D42 the pluripotency genes decreased in both cultures, but to a greater degree in the laminin-coated scaffold cultures compared to non-coated scaffold cultures (Figure 5A, B). The unexpected continued expression of NANOG and OCT4 prompted closer examination of the expression of these genes in the early weeks

of culture. NANOG expression in both coated and non-coated scaffold cultures increased above baseline and peaked at D21 and then downregulated, with significantly decreased expression at D42 (Figure 5C). OCT4 exhibited a similar expression pattern, with initial upregulation which peaked at D30 and then decreasing expression (Figure 5D). Persistence of pluripotency genes would be a concern for uncontrolled growth or differentiation. However, our laminin-coated scaffold cultures demonstrated downregulation of NANOG and OCT4 by D42 in culture.
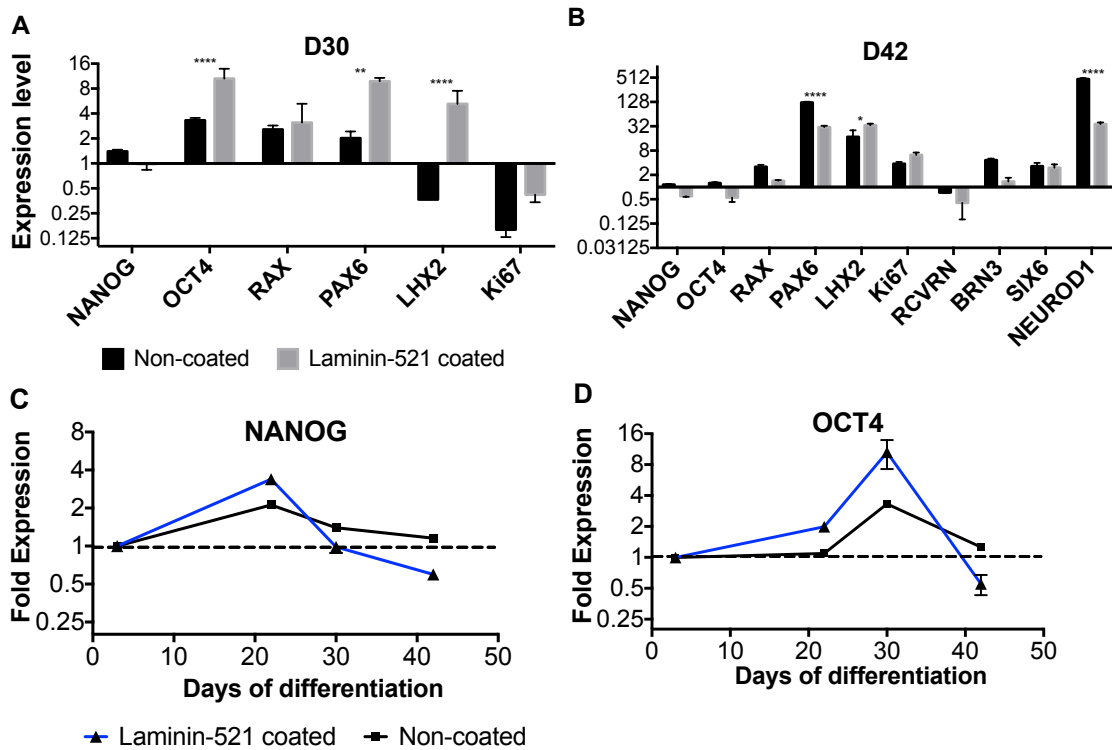
Figure 5. qRT-PCR assay of genes. A) Gene expression at D30 of culture, in L-521 coated and non-coated RPC cultures. B) mRNA levels in D42 cultures. C) Expression of NANOG through 42 days of differentiation. D) Expression of OCT4 with time in differentiation. ± SEM, ****$p < 0.0001$, **$p < 0.01$, *$p < 0.05$

Assessing gene expression of GCH-L521 RPCs at D61, NANOG and OCT4 were significantly downregulated at that time, and retinal specifying genes were upregulated to indicate appropriate differentiation (Figure 6).


Figure 6. RPC differentiation at D61 on GCH-L521. NANOG and OCT4 were significantly downregulated. ± SEM
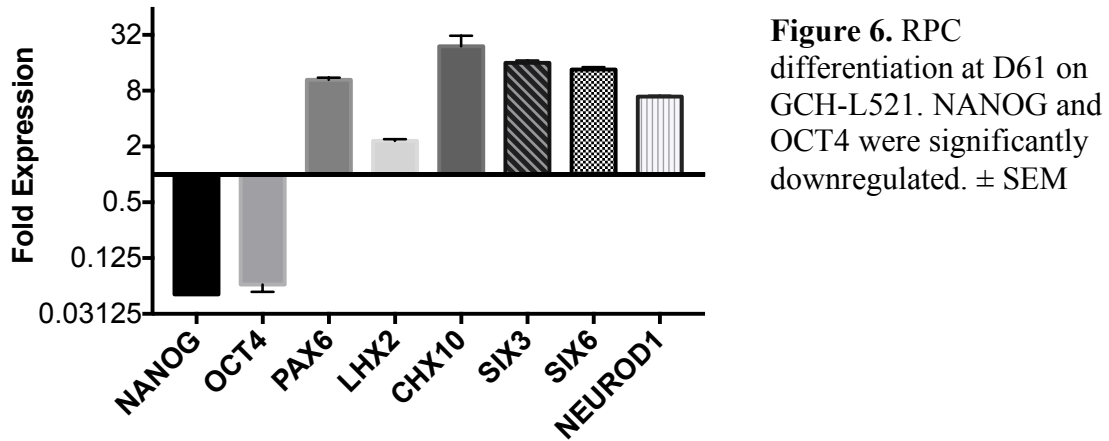
RPC protein expression of retinal differentiation markers

Immunofluorescence assays were carried out to monitor expression of appropriate retinal differentiation proteins in RPCs cultured on GCH-L521 scaffold. Figure 7 shows an example cross-sectional stain of RPCs on the planar scaffold. The scaffold autofluoresces in each color channel. At D42, RPCs on GCH-L521 expressed the early eye field markers PAX6 and LHX2, consistent with qRT-PCR data. At lower magnification, one can discern pockets of RPCs where one gene is expressed greater than the other, i.e. brighter fluorescence of one marker (Figure 7A). This patterning may indicate active differentiation of RPCs into the varying types of retinal cells. Further along in culture, RPCs expressed markers indicative of continued specification of RPCs. CRX and OTX2 are both homeobox proteins that contribute to photoreceptor differentiation from progenitor cells during development [67-69]. RPCs on GCH-L521 began expressing CRX and OTX2 by D51.

D 42
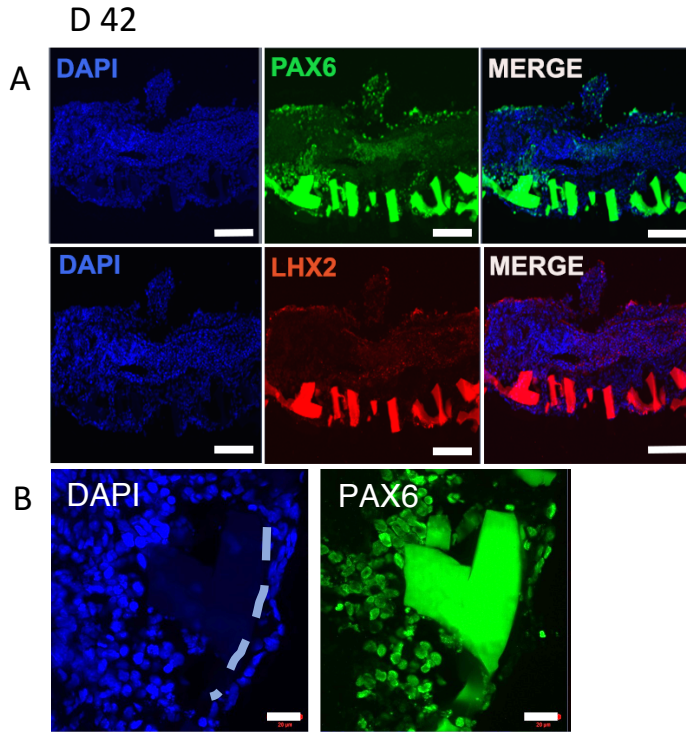
Figure 7. D42 RPC on GCH-L521 scaffolds. A) 10x images; scale bar 50µm. Homogenous fluorescence is the autofluorescent scaffold. B) 40x images; scale bar 20µm. Dotted line demarcates the bottom edge of scaffold.

D 51
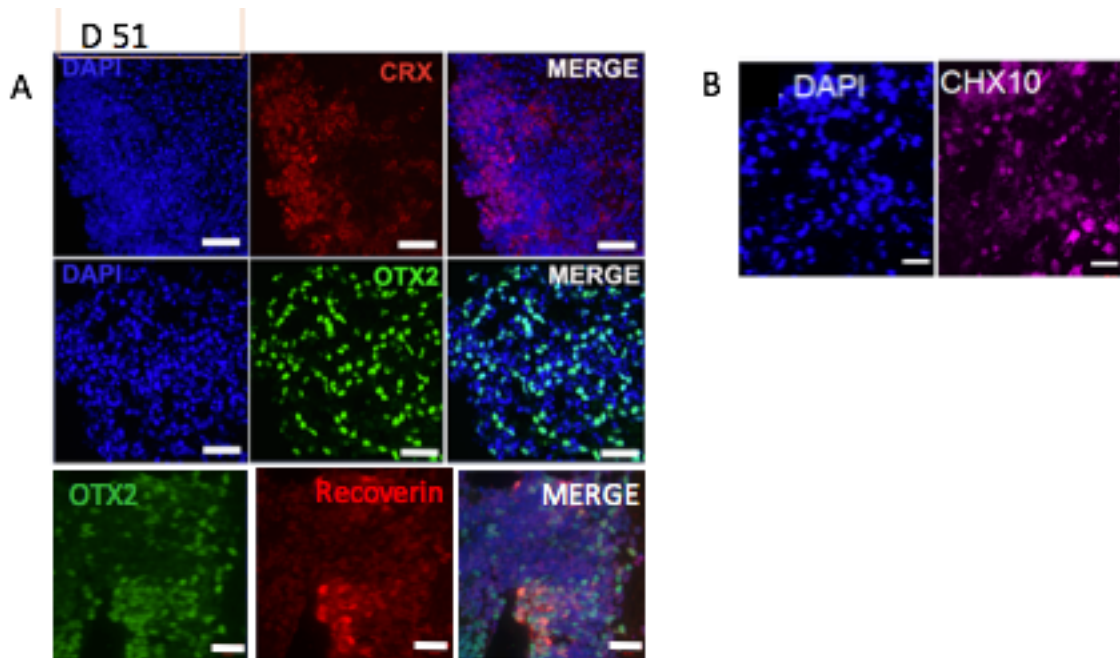
Figure 8. D51 RPC on GCH-L521 scaffold. A) photoreceptor differentiation with CRX, OTX2 and recoverin expression; co-localization of OTX2 and recoverin. Scale bar, 20µm. B) CHX10 expression, suggesting bipolar cell specification. Scale bar, 20µm.

Recoverin, a photoreceptor protein, was also expressed by RPCs and co-localizes with OTX2 (Figure 7A).

CHX10 is a factor expressed early in retinal development to maintain RPC proliferation and subsequently mediates bipolar cell differentiation [70, 71]. RPCs on GCH-L521 expressed CHX10 at D51, suggesting differentiation into retinal interneurons (Figure 8B). By D77 in culture, additional markers of inner retinal layers were expressed (Figure 9). HuC/D is a protein expressed in developing ganglions, horizontal and amacrine cells [72, 73], and BRN3 is a ganglion cell marker [72]. Photoreceptor remain differentiated as demonstrated by the expression of rhodopsin (Figure 9).
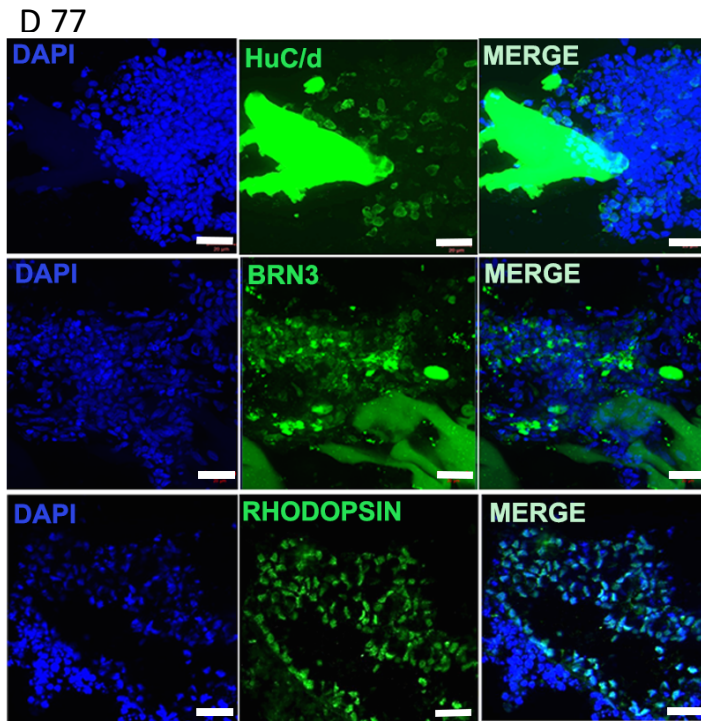
Figure 9. D77 RPC on GCH-L521 scaffold. HuC/D indicates interneuron differentiation. BRN3 is a ganglion cell marker. Rhodopsin is a photoreceptor marker.

Immunoblot assays confirmed the immunofluorescence data of early cell cultures. In very early D3 cultures, LHX2, PAX6, recoverin and BRN3 were at undetectable levels. However, all four proteins were upregulated by D71 (Figure 10).
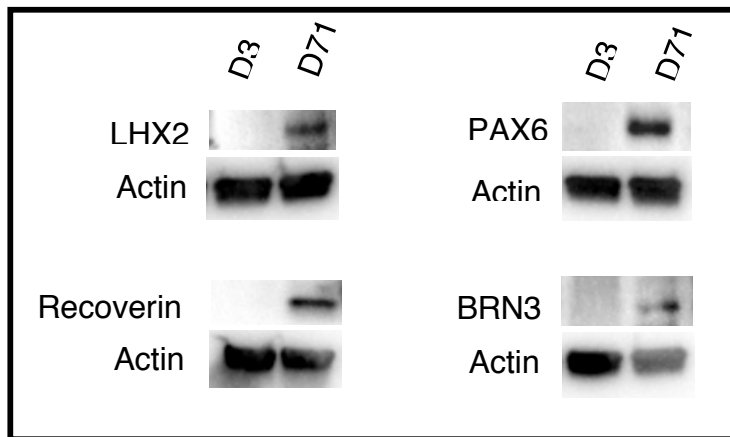
Figure 10. Immunoblot of retinal differentiation proteins. Actin blotted as control.

Segregation of RPC into retinal cell types

Basement membranes are critical parts of tissue structure because they provide cell adhesion points and regulate cell organization. The ILM has been shown to mediate retinal lamination and Müller cell organization [37, 74, 75]. Our hypothesis is that the laminin-521 coated scaffold, can act effectively as an ILM, and induce self-organization and lamination of the cultured RPC. In some RPC clusters cultured on GCH-L521, specific cell types began to segregate, forming gross laminations. Recoverin+ cells (photoreceptor-like RPCs) segregated from BRN3 (ganglion cell-like RPCs) (Figure 11A). In other clusters, recoverin+ cells formed distinct layer from LHX2+ cells (likely differentiating Müller cells) (Figure 11B). It is important to note that such gross lamination was not observed consistently in every RPC cluster cultured on laminin-coated scaffold.
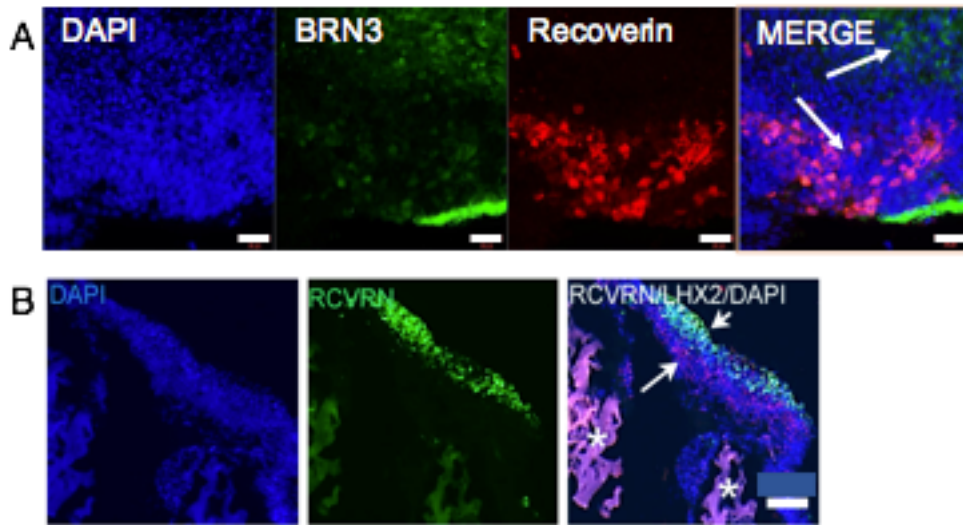
Figure 11. Gross RPC laminations observed in some cell clusters. A) BRN3+ cells segregating from recoverin+ cells. Scale bar, 20μm. B) Recoverin+ (green) cells layering next to LHX2+ (magenta) cells. Scale bar, 50μm.

RPC scaffold cultures preserved more nuclei in degenerating photoreceptors

A transplantable tissue ideally will survive and integrate with the host retina to establish functional connections with host cells. RPCs cultured on laminin-521 coated GCH scaffold were transplanted into RD10 mice to assess the effect of the graft in a degenerating retina. The RD10 mouse model contains a mutation in a rod-phosodiesterase gene (PDE6B) that causes photoreceptor death and subsequent inner retinal degeneration [76, 77]. RD10 mice provides a model of autosomal recessive retinitis pigmentosa (RP) in humans. Degeneration begins around three to four weeks after birth with rapid loss of photoreceptors in the outer nuclear layer (ONL).

After retinal cups containing RPC have differentiated on GCH-L521 scaffold for three weeks, scaffold cultures were transplanted subretinally in RD10 mice on postnatal day 30 (P30). Eye tissue was collected ten weeks after transplantation (P100). By that time, the scaffold appeared to have biodegraded, with no fluorescence evidence on microscopy. Transplanted RPC survived in the host retina and could be identified with TRA-1-85, a

marker for human-derived cells (Figure 12). The RPC also stained positive for recoverin

indicating that the transplanted cells maintained their differentiation. As a control, no TRA-

1-85+ cells were found in the non-transplant eye as expected. By 14 weeks of age (time of

tissue harvest), the ONL of RD10 mice has degenerated to a single layer of photoreceptors

(Figure 12, control). In the transplant eye, more photoreceptor nuclei were present at the

transplant site. The transplanted TRA-1-85+/recoverin+ cells contributed to the ONL

(Figure12, transplant), indicating the ability for the scaffold graft to mitigate the cells loss

in retinal degeneration.
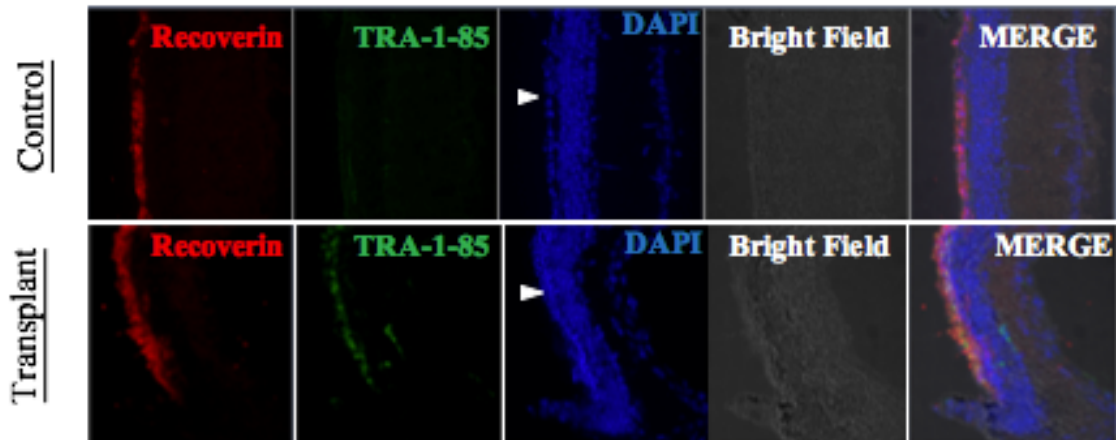
Figure 12. Transplanted RPCs in RD10 mouse retina, identified by TRA-1-85 (human cell marker). Tissue analysis done at 10 weeks post-transplantation. Recoverin stains for photoreceptors, which compromises the outer nuclear layer (ONL) of the retina. Arrow heads point to the number cell nuclei in the ONL.

In some regions of the transplant area, transplanted RPCs were observed to have

migrated deeper into the host retina. TRA-1-85+ cells moved into the inner nuclear layer

(INL), where horizontal, amacrine, and bipolar cells are located, and into the inner

plexiform layer (IPL), which is composed of dendrites of ganglion cells (Figure 13). The

TRA-1-85+ cells that migrated into the inner retina were not recoverin positive, suggesting that these migrating RPC were likely of another retinal cell lineage than photoreceptors.
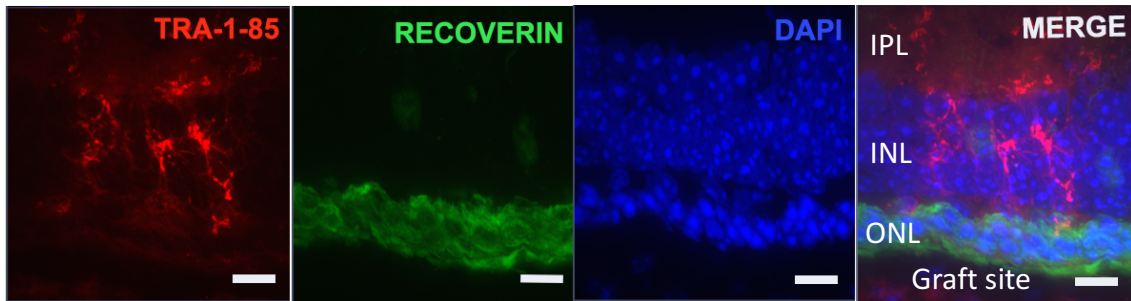
Figure 13. Transplanted RPCs migrating from graft site into the inner retina. 10 weeks post-transplantation. ONL- outer nuclear layer; INL- inner nuclear layer; IPL- inner plexiform layer. Scale bar, 10μm.

To assess for changes in visual function, multifocal electroretinogram (mfERG) were measured on the transplanted RD10 mice. ERG measures the electrical signals from the retina in response to light stimulation. The ERG can be used to monitor retinal degeneration as signal transduction becomes slower and lower in amplitude [77]. mfERG is a variation of this testing where electrical activity can be correlated to specific areas of the retina. We measured the mfERG of RD10 mice before after transplantation to evaluate for any functional recovery (Figure 14). A characteristic mfERG waveform is shown in Figure 14B. The N1 peak correlates to photoreceptor activity after a light stimulation, and the P1 peak correlates to transmission of signal to the bipolar cells in the inner retina. Proper photoreceptor function is necessary for robust P1 waves. As expected, our data shows that at time of transplantation (post-natal day 30, P30), P1 amplitude is similar to wild-type (WT) because degeneration is in the early stages. Four weeks post-transplantation, mfERG was measured again, showing significantly decreased amplitudes in both the transplanted and non-transplanted eye (Figure 14C). Additionally, there was no
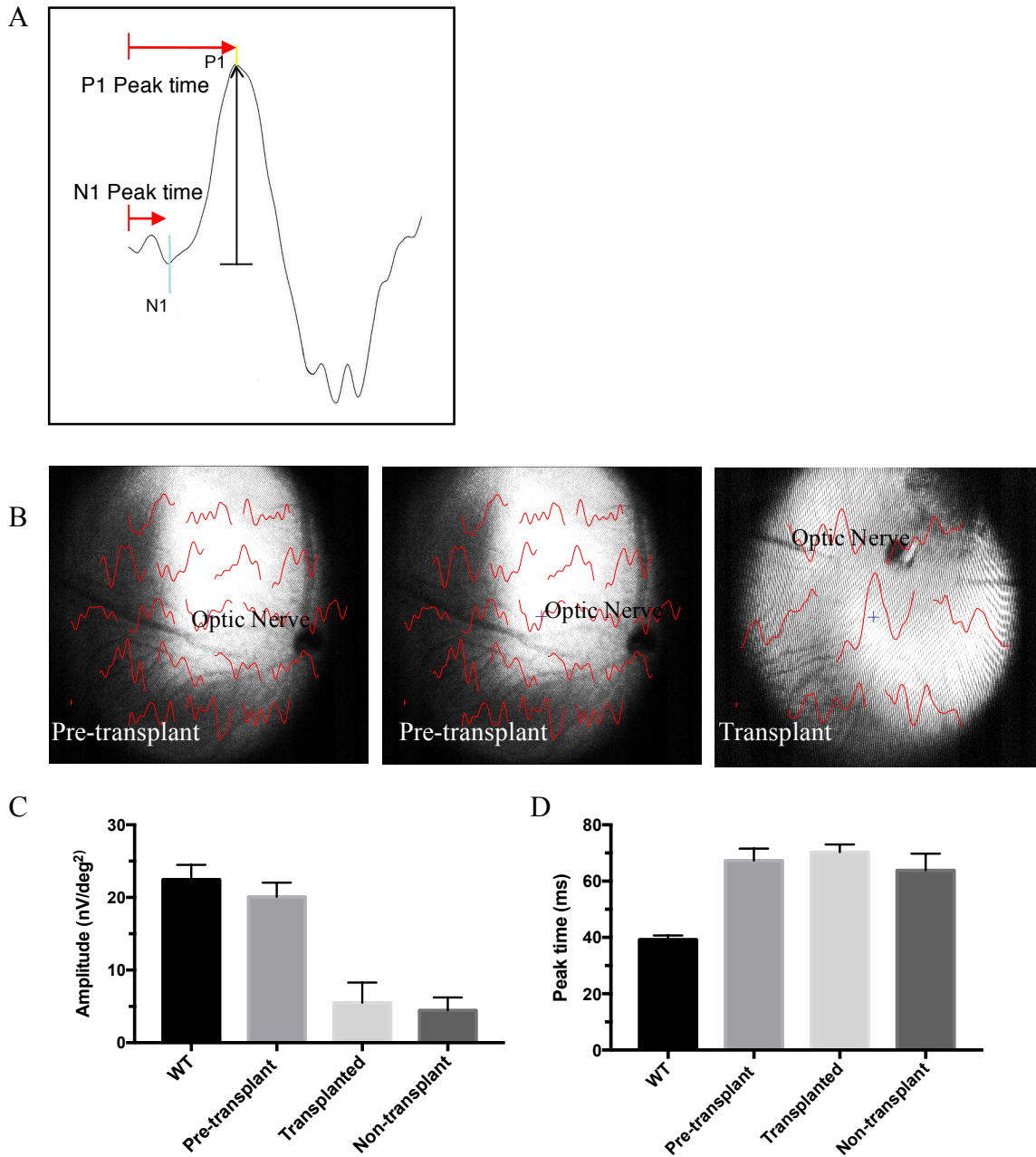
Figure 14. mfERG of RD10 mice before and after transplantation. A) Idealized mfERG waveform. Adapted from Dutescu et al. (*89*) B) Representative fundus photograph of area of retina where measurements were taken. C) P1 wave amplitude, values of the measurement area were averaged D) Peak time of P1 wave; values of measurement area were averaged. Pre-transplant measurement taken at post-natal day 30 (P30). ± SEM

significant difference between the transplanted eye and the non-transplanted eye. Peak time is another informative parameter in ERG measurements. It is the time from the onset of light stimulus to the peak wave amplitude. This time measurement is an indication of the signal transduction within the retina and can become delayed in retinal disorders when neuronal connections are disrupted [77, 78]. In our experiment, the peak time was already delayed at the time of transplantation compared to WT. Repeat measurement four weeks later did not show significant changes in peak times, in either the transplant or non-transplant eyes (Figure 14D).

Preliminary data on good tolerability of GCH-L521 scaffold in pig eyes

For a retinal graft to be ultimately used in human treatments, it is ideal to conduct transplantation studies in large animals, whose eyes are more anatomically and physiologically similar to human eyes. Results from large animal studies can allow further optimization of retinal grafts. We began a pilot study transplanting RPCs scaffold grafts into normal pig eyes. The initial aim of the pilot study was to evaluate whether our immunosuppression protocol was sufficient to control the pig immune reaction against the RPC xenograft. Data has been collected from eight transplantation procedures so far: four animals received RPC on GCH-L521 scaffold, one animal received only GCH-L521 scaffold with no cells, another one received only polyester (PET) transwell filter, one animal received hESC-derived RPE on PET filter, and the last animal received a co-culture of RPC and RPE. Table 1 provides the details of each animal surgery.

Mild redness and swelling of the conjunctiva was present immediately following surgical procedures, but typically resolved completely after two days. Subsequently on

daily monitoring, no animals showed gross signs of ocular inflammation, such as enlarged blood vessels on the conjunctiva or sclera, hazy cornea, or debris in the anterior chamber. On histology, mild folding of the retina was observed mainly around the transplantation region (Figure 15). Additionally, no infiltrating cells or granulomas were present; the architecture of retinal layers remained fairly intact. To assess immune reactivity at the tissue level, retina tissue sections were stained for IL-6 and IBA-1. IL-6 is a cytokine that is highly expressed in inflammation and during graft rejection, and IBA-1 is a marker for microglia, which can assess for increased immune reactivity [79, 80]. The scaffold was placed to lay flatly between the retina and the RPE/choroid. I examined the two sides of the graft on immunofluorescence, one side abutting the retinal ONL and the other abutting the choroid. There was no significant difference between IL-6 staining between the transplanted and the non-transplanted control eye, indicating no upregulation of the inflammatory marker (Figure 16). In the control eye sections, IBA-1 staining identified the resident microglia cells within the choroid and retina (Figure 16). In transplanted eyes, IBA-1 positive staining appears mildly increased on the choroid side but not significantly increased on the retina side compared to control eye. No adjustment of our immunosuppression protocol was made. In the animals that received RPC on GCH-L521 scaffolds, few TRA-1-85+ cells were found at the transplant site (Figure 17). Compared to the quantity of RPCs transplanted initially, there was significant cell loss at 22 days after transplantation.

Complications were observed mainly at the tissue level on dissection (Table 1). As mentioned above, the most common complications are mild scarring and wrinkling of the retina around the transplantation site (Figure 15) and vitreous debris. Less common, but

more serious complications were retinal detachment and lens opacification; both were most likely caused by inadvertent trauma during the surgical procedure. The two latter complications prevented imaging and mfERG measurements on follow-up in three animals.
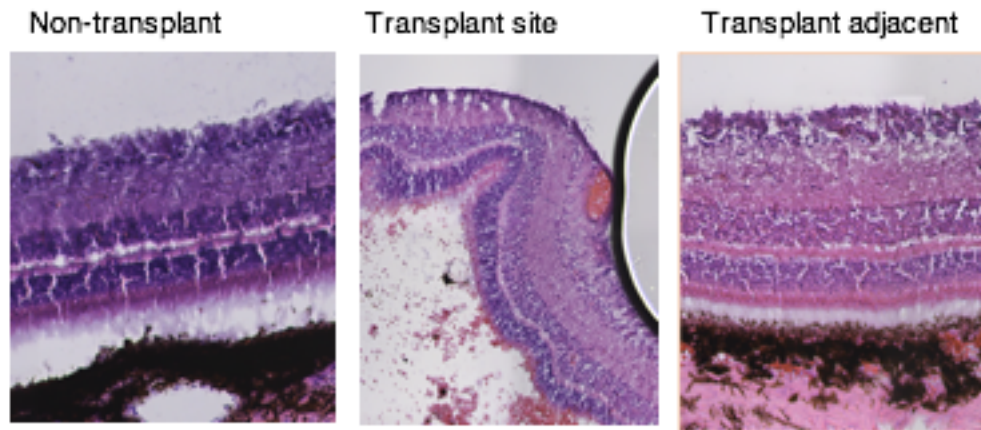
Figure 15. H&E stain of pig retinal sections. Non-transplant section shows retinal architecture of the non-operated eye. Transplant site is where the scaffold was inserted. Transplant adjacent is the areas around the insertion site, where retinal architecture remained normal.
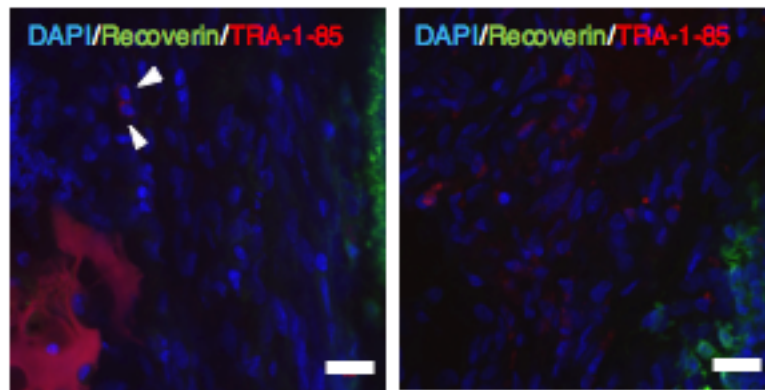
Figure 16. Few transplanted RPCs (TRA-1-85+) found around the graft transplantation site. TRA-1-85+ cells were not positive for recoverin. Scale bar, 20μm.
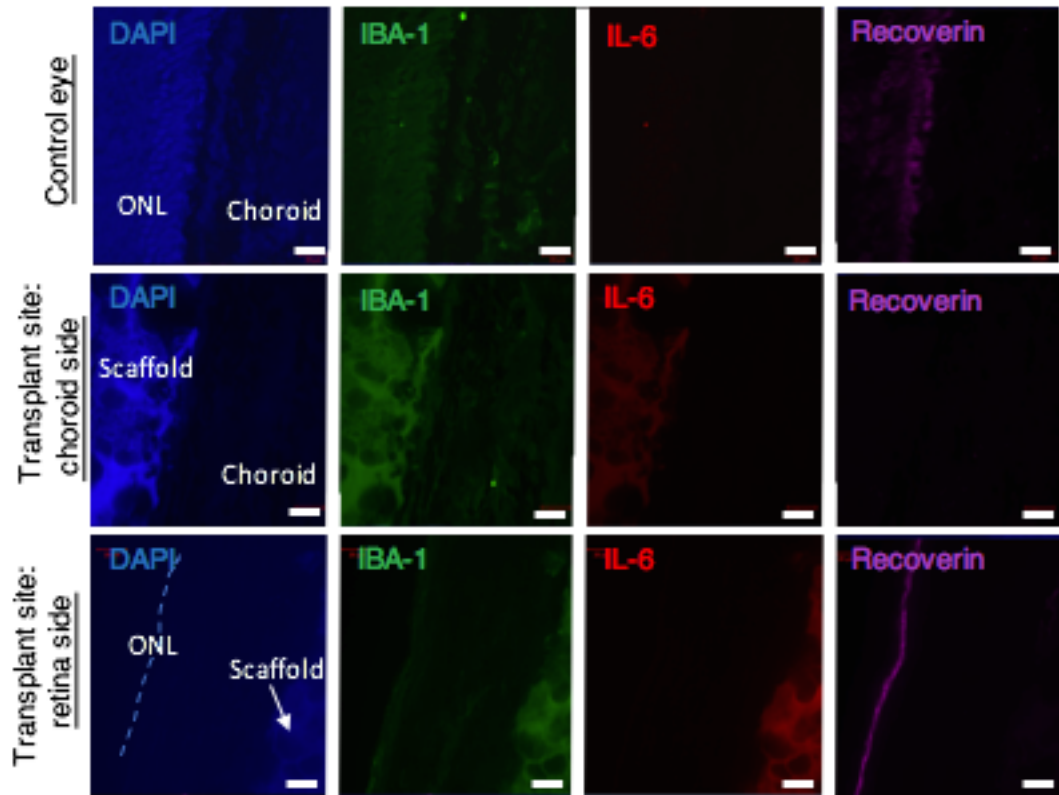
Figure 17. Immunoreactivity of scaffold in the host retina. Representative immunofluorescence sections. Scaffold was inserted flatly between the retina and choroid. IBA-1 and IL-6 positivity was assessed on both sides of the scaffold. Recoverin identifies the host photoreceptor layer. Scale bar, 20µm.

TABLE 1

Animal	Scaffold material	Follow-up period	Immunosuppression	Complications
332	-Transwell PET filter -No cells	Immediate collection	None	N/A
344	-GCH -No cells	12 days	-Triamcinolone (intraocular) 1mg/eye	-Gross pathology: Posterior lens opacification Large retinal detachment Vitreous scarring/traction
358	-GCH-L521 -D16 EBs	8 days	-methylprednisone 2mg/kg IM (pre-op, once) -Triamcinolone (intraocular) -Prednisone 2mg/kg PO daily	- Gross pathology: Vitreous hemorrhage and scarring
369	-GCH-L521 -D71 RPCs	15 days	Same as above (#358)	-Gross pathology: Trace vitreous debris No major complications
374	-GCH-L521 -D37 RPCs	22 days	Same as above	-No major complications
376	-GCH-L521 -D23 RPCs	22 days	Same as above	-Gross pathology: Vitreous debris Mild retinal scarring
382	-hESC-RPE on PET filter	20 days	Same as above	-Gross pathology: Posterior lens opacification Vitreous debris Retinal scarring
383	Co-culture: -D56 RPC on GCH-L521 -hESC-RPE on PET filter	29 days	Same as above	-Gross pathology: Mild retinal scarring at transplant site

Table 1. Summary of pig retinal transplantations. Grafted cells and scaffold, follow-up length, immunosuppression regimen, and complications are listed. PET- polyester; IM- intramuscular; PO- per os (by mouth).

Challenges in pig retinal transplantation

Our preliminary results suggested the immunosuppression was sufficient and the GCH-L521 scaffold has good biocompatibility. A secondary goal of the pig project was to optimize mfERG measurements of pig eyes in order to monitor in visual function after the surgical procedure. Previous work in the Rizzolo lab conducted mfERG measurements of pig retina after laser injury and was able to distinguish the light sensitive visual streak from non-visual streak areas of the retina (YSM Thesis of Laurel Tainsh). We attempted to measure mfERG before and after intraocular transplantation procedures. The major challenge was reducing the environmental interference that contributed to the background artifact of the measurements. The best attempt was made to block interfering electromagnetic fields: animals were covered with a field shielding blanket, and all unnecessary electronics were turned off during measurements. However, because we could not shield the entire surgical room and the sedated animals must continue to be monitored on the ventilator, the existing artifacts contributed to inconsistent mfERG measurements. This inconsistency hindered comparison of measurement values from before to after the transplantation (see Figure 19A).

Another challenge to acquiring consistent and reliable mfERG was the difficulty in positioning the pig's eye for imaging. Unlike human subjects who can be instructed to look in specific directions to image a particular area of the retina, this was not possible in sedated animals. Occasionally, superficial sutures were put through the sclera of the animal to pull the eye in desired directions; however, even with manipulation of the animal's eye, there could be significant movement during the measurement period, contributing to unreliability of the recordings. Similarly, on follow-up after transplantation, it was

sometimes difficult to position the eye to access the same area of the retina measured on a previous test. Figure 19B shows an example of good mfERG measurements taken before and after transplantation in an animal, however, the region of the retina that was measured did not correspond closely, limiting subsequent comparison.

OCT is a non-invasive imaging modality that captures cross-sectional images through the retina and allows evaluations of retinal tissue architecture, similar to ultrasound images. OCT is potentially very useful in retinal transplantation studies because it is a quick study and can reveal signs of complications without having to collect tissue. Figure 18 shows an example of mild retinal folding at the scaffold transplantation site, but no major retinal detachments. However, the difficulty with positioning was also a major challenge in using optical coherence tomography (OCT) to monitor transplanted graft *in vivo*. It was difficult to obtain consistent OCT images of the same area in the retina on subsequent follow-up tests.
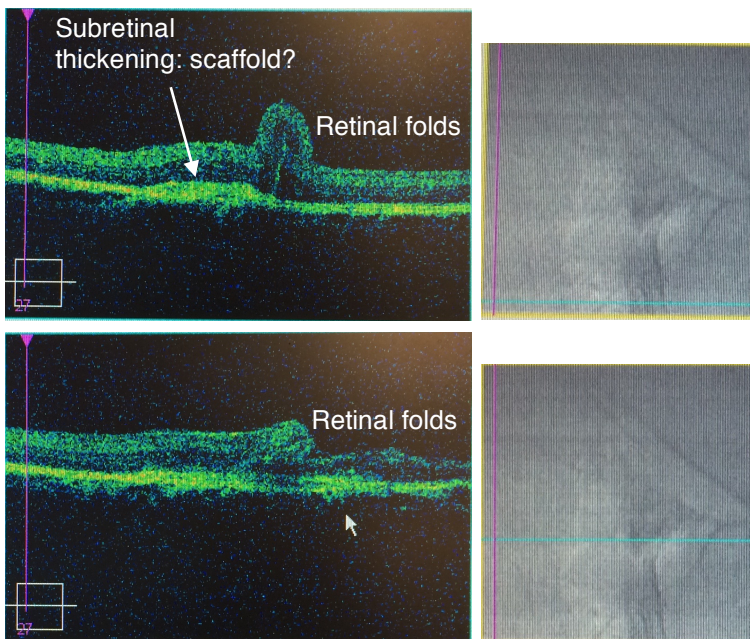
Figure 18. Example OCT images. Changes in retinal architecture can be imaged, including retinal folds, retinal or subretinal thinning or thickening. Images on right are the fundus photograph of the imaged area. Blue line- where cross-sectional image (left) is located.
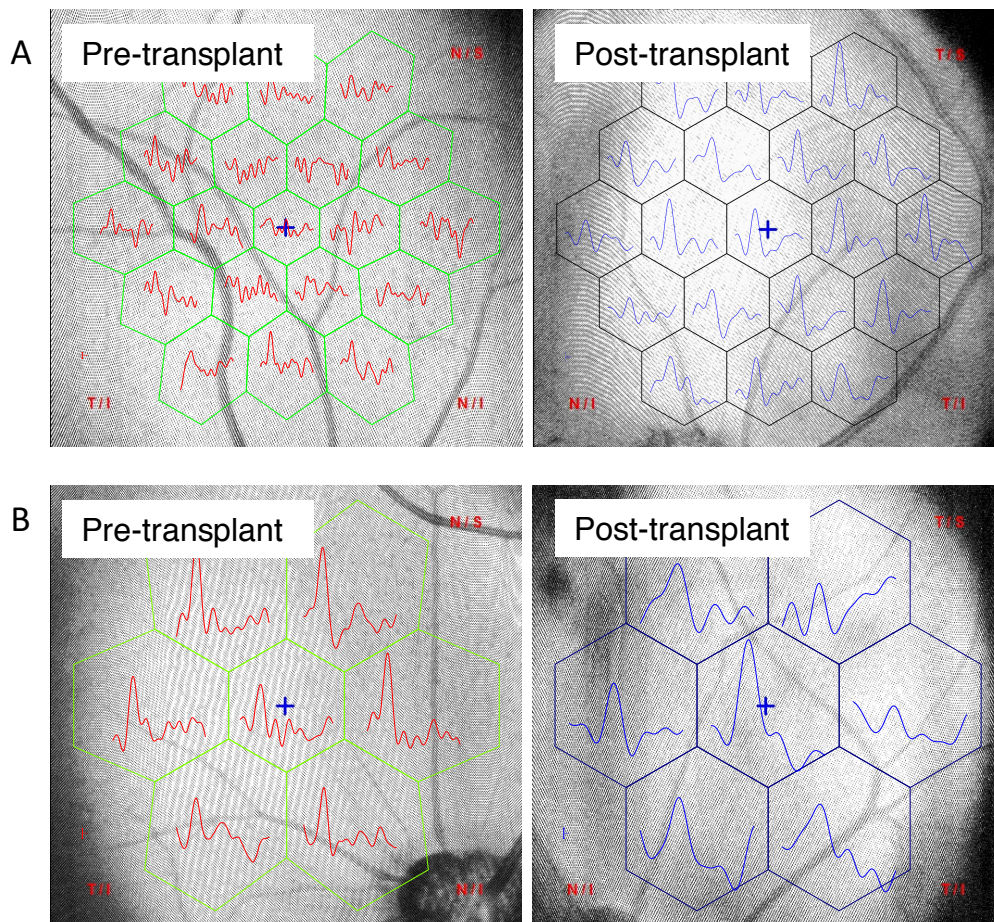
Figure 19. Example mfERG recordings. A) Inconsistency in controlling background signal noise. Pre-transplant mfERG noisier and lower than post-transplant measurements. B) Challenge in consistent positioning. Good pre- and post- transplant measurements, but difficult to align to the same retinal location.

Besides overcoming the technical challenges of large animal studies, the surgical capacity of the animal facilities is also important in obtaining meaningful data in an efficient way. This pilot study was the first large animal retinal transplantation study carried out at Yale University. The Yale Animal Resources Center (YARC) provided the veterinarian and anesthesia support for the surgical procedures. Veterinarians were also consulted on the appropriate drugs for pain control and alternative sedation medication to

optimize mfERG recordings. One main limitation was the low operational capacity of the animal facility. Due to the time required for mfERG and OCT measurements, one survival animal procedure can realistically be done in a single day; and commonly one to two survival procedures can be done in a week, given personnel availability and facility regulations. The low capacity slowed the optimization process for the surgical procedure and data collection. Moving forward, increasing the number of procedures per week would allow experimenters to become even more facile with the transplantation procedure and to implement timely experimental adjustments as needed.

DISCUSSION

Retinal degeneration, such as retinitis pigmentosa and AMD, are debilitating disease causing visual impairment and blindness. Currently, there are no treatments that effectively reverse disease or can replace dying retinal tissue. The ability to differentiate stem cells into retinal cells holds promise for developing transplantable grafts that can lead to vision recovery. More research is investigating the use of scaffolds to culture retinal progenitor cells (RPCs) for transplantation. The mechanical and physical properties of the scaffold, such as stiffness, elasticity, and having nanowires or grooves, can be modified to improve the efficiency of the differentiation process [34, 35]. Another advantage of using scaffolds is possible higher retention of cells during transplantation. Currently, many transplantation studies including human clinical trials implant cells by injecting a cell suspension [19, 50, 81] . However, this method leads to significant cell loss, either from reflux of cells during injection or cell death due to lack of connection with other cells while in suspension. A scaffold model would not only allow cells to remain adherent but also support synaptic connections between developing neural retinal cells. Subsequently, the entire composite graft can be transplanted subretinally.

Previous studies of retinal cultures on scaffold mostly studied RPE cultures, and scaffolds attempted to mimic the RPE basement membrane composition. Our scaffold model is unique because it attempts to culture human ESC-derived RPC on a scaffold with 3-dimensional depth. The novel scaffold is synthesized from gelatin, chondroitin sulfate and hyaluronic acid to closely mimic the compositional ratio of the natural extracellular matrix (EMC) of the retina [82]. The aim of the culture model was to coerce the RPCs to use the 3-D structure of the scaffold to self-organize into the natural layers of the retina.

However, initial results from our lab showed that RPCs did not readily migrate into the depth of the scaffold; most RPCs remained clustered on top of the scaffold [36]. My project sought to address this limitation by modifying the scaffold further by coating it with laminin-521. Existing studies on scaffold cultures coated them with ECM, including laminin and collagen, to mimic the natural retinal ECM and increase cell adherence [29, 34]. Similarly, we hypothesized that laminin-521 would increase RPC attachment on the GCH scaffold. Additionally, because laminin-521 is the dominant laminin of the ILM, it may provide a basement membrane signal and direct tissue organization.

Our data demonstrated that the laminin-521 coated GCH scaffold improved cell attachment and migration within the scaffold. Higher cell retention in culture increases the yield of differentiating retinal cells, which enables more experimentations and data collection. The laminin-521 modification increased cell migration to populate the entire thickness of the scaffold and is an important first step toward achieving a 3-D self-organizing retinal tissue culture.

Importantly, the RPCs seeded onto GCH-L521 scaffold continued to differentiate and expressed developmental markers of different interneurons within the retina. Photoreceptors had begun developing by day 51 in culture, and there was also evidence of differentiating bipolar cells at that time. By day 77, differentiating ganglion cells began to appear within the scaffold culture. Interestingly, the pluripotency markers NANOG and OCT4 were expressed to significant levels into day 30. In other studies, expression of pluripotency gene decreased earlier in the retinal differentiation process [19, 22]; one study demonstrated that ESC differentiated into neural phenotype with significant downregulation of OCT4 by four weeks in culture [19]. The continued expression of

NANOG and OCT4 may be an effect of the laminin-521 modification. Laminin-521 is found in abundant levels in the stem cells niche of human ESCs as well [83, 84]. In culture, the laminin-521 substrate contributes to the maintenance and expansion of ESC, and it is now commercially available for growing ESC cultures [84]. Therefore, in the context of the blastocyst in embryonic development, laminin-521 may play a role in maintaining the pluripotency of ESCs. This property could explain the persistence of NANOG and OCT4 in our cultures during RPC differentiation. Having undifferentiated cells can be a concern for possible uncontrolled cell growth, however, our results demonstrated that by day 42 in differentiation media, both pluripotency markers were significantly downregulated, with continued expression of appropriate retinal markers.

We hypothesized that laminin-521, a component of the ILM, would provide a developmental signal to promote lamination of RPCs within the scaffold. Gross laminations were observed in some RPC clusters on the scaffold, where developing photoreceptors are segregating from the ganglion cell precursors. The RPCs are beginning to form a composite graft within the scaffold with polarity of the natural retina. For AMD and retinitis pigmentosa, degeneration begins in the outer retina, in the RPE and photoreceptor layers, respectively. As disease advances, the inner layers become affected as well, with remodeling and retraction of neuron processes and death of the inner retina [77, 85, 86]. To treat advanced retinal diseases, an ideal graft would have the ability to replace the different types of degenerating cells. Our results indicated an important step toward achieving this goal.

In the mice transplantation experiments, the RPC scaffold graft demonstrated biodegradability and continued RPC survival in the host retina. Biodegradability is a useful

feature of scaffolds because it provides mechanical protection during the culture and transplantation process but can gradually degrade to allow RPCs to generate their own ECM and integrate with host cells. At 10 weeks post transplantation in RD10 mice, the scaffold had degraded and grafted RPC contributed to the native photoreceptor layer. Structurally, the transplantation was able to replenish the cells lost from degeneration. Additionally, some RPCs were observed to migrate deeper in the host retina. The migrating cells were not maturing photoreceptors because they did not express recoverin; therefore additional retinal markers need to be assayed to identify the migrating cells. It can be hypothesized that those cells were differentiating into neurons of the inner nuclear layer and were homing to the appropriate layers of the host retina. We also did not assay for functional integration of the transplanted RPCs. As a future experiment, tissue sections can be stained for synaptic proteins, such as α-transducin and PSD-95, to detect any synaptic integration between grafted and host cells [87, 88].

It is known that photoreceptor loss increases significantly after 1 month of age in RD10 mice [77]. Therefore, we implanted the GCH-L521 RPC grafts when degeneration had begun in order to test for any functional recovery from our transplantation. On our functional testing in the transplanted RD10 mice, the mfERG did not show an effect from the implantation. Additional work, both in graft culture and functional testing, needs to be done to achieve the goal of demonstrating functional visual recovery. mfERG is a relatively new method for measuring retinal function in rodent studies. More commonly, a full-field ERG is used to assess visual function, which calculates a summary electrical signal from the entire stimulated area. mfERG divides the stimulated area into smaller segments and measure the retinal signal, so that signal waveforms can be correlated to specific stimulated

areas (Figure 19). This feature is useful for evaluating the efficacy of transplantation because the implantation area is relatively small within the whole retina. Therefore, mfERG would be able to discern changes in retinal function specifically at the transplant site, which may not be discernable if full-field ERG were used. However, a trade-off to having geographic specificity is that the measured signals are weaker, which often requires recordings over several minutes. The parameters for applying mfERG to mice is still being optimized, such as stimulus frequency and intensity, and landmarks for visualization [89]. To improve on our RD10 mouse mfERG measurements, mfERG monitoring can start earlier and more frequently to detect any small effects of the procedure. One technical change that may improve mfERG measurements and reduce background noise is to record ERG signals for up to 10 minutes [89]. Additionally, new instrument hardware is available that can provide higher intensity of the stimulation light, which may improve the retinal response and the mfERG signals.

To move research toward human treatments, large animal studies can lead to further optimization of therapeutic methods because of increased anatomical and physiologic similarity to human tissues. Previous studies of retinal transplantation in pigs implanted RPE cells or RPCs that were in suspension, with good tolerability, graft survival and possible integration of transplanted cell within the host [56-58, 90]. Our pilot study tested the feasibility of transplanting a 3-D RPC scaffold graft and controlling the adverse effects of the procedure. The preliminary data indicated good tolerability of the graft with no significant difference in immune reaction between the transplanted and non-transplanted eye. Our immunosuppression protocol, one dose of prednisone a week before surgery and daily prednisone (2mg/kg) after surgery, was sufficient to control any inflammatory and

immune processes. Immunosuppression was needed in our study because we transplanted cells derived from human ESC. Our implanted cells did have limited migration into the host retina. However, this may be due to the short follow-up period for tissue analysis; our experiments did not go past four weeks post-transplantation. At that time, the scaffold had not degraded in the subretinal space, and may be limiting the interaction between grafted and host cells.

As discussed in the results section, the pig transplantation study encountered several technical challenges. The complications associated with surgery was expected as part of the learning curve of a large animal study, and were quickly minimized with increased experience. However, obtaining consistent and valid measurements on mfERG and OCT were larger challenges to overcome. Additional methods of reducing signal artifacts need to be tested to gain reliable mfERG readings. For example, more extensive electromagnetic shielding of the operating room may be required to reduce background noise [91]. Also obtaining mfERG immediately after anesthesia of the animal may also improve quality of measurements [91].

The long-term goal of this project is to develop a viable retinal graft capable of restoring visual function. An ideal graft would include all the cell types lost in the degenerative process. With our initial success in culturing RPC on a 3-D scaffold, our lab is exploring the effects of co-culturing the RPC scaffold culture with a RPE monolayer. Reciprocal interaction between RPE and developing RPCs may facilitate further maturation of retinal cells than monoculture alone. Bruch's membrane, the basement membrane on the basal side of RPE cells, has also been shown to play a role in retinal development. In the developing chick retina, Bruch's membrane promotes proper

polarization of membrane proteins in RPE cells [92]. Indeed, flat polymer scaffolds have been synthesized to mimic Bruch's membrane to better culture RPE cells [93-95]. As a future direction, we can consider co-culturing our 3-D RPC scaffold graft with RPE monolayers cultured on synthetic Bruch's membrane, to form a graft that mimics native retina even more closely. Additionally, the ability to generate tissue similar to native retina in culture offers the possibility for more effective pharmacologic testing *ex vivo* before moving to animal studies.

Overall, this project demonstrated that a novel laminin-521 coated porous scaffold can support growth and differentiation of ESC-derived RPCs. RPC GCH-L521 grafts were able to survive in the subretinal space of RD10 mice and exhibited some degree of migration within the host retina. These scaffold cultures can also be translated into studies in larger animals, demonstrating good tolerability of such a 3-D RPC scaffold graft.

REFERENCES

1. Kimbrel, E.A. and R. Lanza, *Current status of pluripotent stem cells: moving the first therapies to the clinic.* Nat Rev Drug Discov, 2015. **14**(10): p. 681-92.
2. Feldman, E.L., et al., *Intraspinal neural stem cell transplantation in amyotrophic lateral sclerosis: phase 1 trial outcomes.* Ann Neurol, 2014. **75**(3): p. 363-73.
3. Lunn, J.S., et al., *Stem cell technology for neurodegenerative diseases.* Ann Neurol, 2011. **70**(3): p. 353-61.
4. Mead, B., et al., *Stem cell treatment of degenerative eye disease.* Stem Cell Res, 2015. **14**(3): p. 243-57.
5. Reichhart, N. and O. Strauss, *Ion channels and transporters of the retinal pigment epithelium.* Exp Eye Res, 2014. **126**: p. 27-37.
6. Dias, M.F., et al., *Molecular genetics and emerging therapies for retinitis pigmentosa: Basic research and clinical perspectives.* Prog Retin Eye Res, 2017.
7. Ambati, J. and B.J. Fowler, *Mechanisms of age-related macular degeneration.* Neuron, 2012. **75**(1): p. 26-39.
8. Friedman, D.S., et al., *Prevalence of age-related macular degeneration in the United States.* Arch Ophthalmol, 2004. **122**(4): p. 564-72.
9. Age-Related Eye Disease Study 2 Research, G., *Lutein + zeaxanthin and omega-3 fatty acids for age-related macular degeneration: the Age-Related Eye Disease Study 2 (AREDS2) randomized clinical trial.* JAMA, 2013. **309**(19): p. 2005-15.
10. Takahashi, K., et al., *Induction of pluripotent stem cells from adult human fibroblasts by defined factors.* Cell, 2007. **131**(5): p. 861-72.
11. Takahashi, K. and S. Yamanaka, *Induction of pluripotent stem cells from mouse embryonic and adult fibroblast cultures by defined factors.* Cell, 2006. **126**(4): p. 663-76.
12. Denham, M. and M. Dottori, *Neural differentiation of induced pluripotent stem cells.* Methods Mol Biol, 2011. **793**: p. 99-110.
13. Van Hoof, D., K.A. D'Amour, and M.S. German, *Derivation of insulin-producing cells from human embryonic stem cells.* Stem Cell Res, 2009. **3**(2-3): p. 73-87.
14. Zhang, R.R., et al., *Efficient hepatic differentiation of human induced pluripotent stem cells in a three-dimensional microscale culture.* Methods Mol Biol, 2014. **1210**: p. 131-41.
15. Klimanskaya, I., et al., *Derivation and comparative assessment of retinal pigment epithelium from human embryonic stem cells using transcriptomics.* Cloning Stem Cells, 2004. **6**(3): p. 217-45.
16. Miyagishima, K.J., et al., *In Pursuit of Authenticity: Induced Pluripotent Stem Cell-Derived Retinal Pigment Epithelium for Clinical Applications.* Stem Cells Transl Med, 2016. **5**(11): p. 1562-1574.
17. Peng, S., et al., *Engineering a blood-retinal barrier with human embryonic stem cell-derived retinal pigment epithelium: transcriptome and functional analysis.* Stem Cells Transl Med, 2013. **2**(7): p. 534-44.
18. Carr, A.J., et al., *Molecular characterization and functional analysis of phagocytosis by human embryonic stem cell-derived RPE cells using a novel human retinal assay.* Mol Vis, 2009. **15**: p. 283-95.

19.   Idelson, M., et al., *Directed differentiation of human embryonic stem cells into functional retinal pigment epithelium cells.* Cell Stem Cell, 2009. **5**(4): p. 396-408.

20.   Eiraku, M., et al., *Self-organizing optic-cup morphogenesis in three-dimensional culture.* Nature, 2011. **472**(7341): p. 51-6.

21.   Meyer, J.S., et al., *Optic vesicle-like structures derived from human pluripotent stem cells facilitate a customized approach to retinal disease treatment.* Stem Cells, 2011. **29**(8): p. 1206-18.

22.   Nakano, T., et al., *Self-formation of optic cups and storable stratified neural retina from human ESCs.* Cell Stem Cell, 2012. **10**(6): p. 771-85.

23.   Ohlemacher, S.K., et al., *Generation of highly enriched populations of optic vesicle-like retinal cells from human pluripotent stem cells.* Curr Protoc Stem Cell Biol, 2015. **32**: p. 1H 8 1-20.

24.   Phillips, M.J., et al., *Blood-derived human iPS cells generate optic vesicle-like structures with the capacity to form retinal laminae and develop synapses.* Invest Ophthalmol Vis Sci, 2012. **53**(4): p. 2007-19.

25.   Zhong, X., et al., *Generation of three-dimensional retinal tissue with functional photoreceptors from human iPSCs.* Nat Commun, 2014. **5**: p. 4047.

26.   Osakada, F., et al., *Toward the generation of rod and cone photoreceptors from mouse, monkey and human embryonic stem cells.* Nat Biotechnol, 2008. **26**(2): p. 215-24.

27.   Liu, Z., et al., *Enhancement of retinal pigment epithelial culture characteristics and subretinal space tolerance of scaffolds with 200 nm fiber topography.* Biomaterials, 2014. **35**(9): p. 2837-50.

28.   Lu, B., et al., *Mesh-supported submicron parylene-C membranes for culturing retinal pigment epithelial cells.* Biomed Microdevices, 2012. **14**(4): p. 659-67.

29.   Sorkio, A., et al., *Surface Modified Biodegradable Electrospun Membranes as a Carrier for Human Embryonic Stem Cell-Derived Retinal Pigment Epithelial Cells.* Tissue Eng Part A, 2015. **21**(17-18): p. 2301-14.

30.   Kador, K.E. and J.L. Goldberg, *Scaffolds and stem cells: delivery of cell transplants for retinal degenerations.* Expert Rev Ophthalmol, 2012. **7**(5): p. 459-470.

31.   Pearson, R.A., et al., *Restoration of vision after transplantation of photoreceptors.* Nature, 2012. **485**(7396): p. 99-103.

32.   Assawachananont, J., et al., *Transplantation of embryonic and induced pluripotent stem cell-derived 3D retinal sheets into retinal degenerative mice.* Stem Cell Reports, 2014. **2**(5): p. 662-74.

33.   Tomita, M., et al., *Biodegradable polymer composite grafts promote the survival and differentiation of retinal progenitor cells.* Stem Cells, 2005. **23**(10): p. 1579-88.

34.   Redenti, S., et al., *Retinal tissue engineering using mouse retinal progenitor cells and a novel biodegradable, thin-film poly(e-caprolactone) nanowire scaffold.* J Ocul Biol Dis Infor, 2008. **1**(1): p. 19-29.

35.   Yao, J., et al., *Enhanced differentiation and delivery of mouse retinal progenitor cells using a micropatterned biodegradable thin-film polycaprolactone scaffold.* Tissue Eng Part A, 2015. **21**(7-8): p. 1247-60.

36. Singh, D., et al., *A biodegradable scaffold enhances differentiation of embryonic stem cells into a thick sheet of retinal cells.* Biomaterials, 2018. **154**: p. 158-168.

37. Denes, V., et al., *Laminin deficits induce alterations in the development of dopaminergic neurons in the mouse retina.* Vis Neurosci, 2007. **24**(4): p. 549-62.

38. Mehes, E., et al., *Laminin-1 increases motility, path-searching, and process dynamism of rat and mouse Muller glial cells in vitro: implication of relationship between cell behavior and formation of retinal morphology.* Cell Motil Cytoskeleton, 2002. **53**(3): p. 203-13.

39. Libby, R.T., et al., *Disruption of laminin beta2 chain production causes alterations in morphology and function in the CNS.* J Neurosci, 1999. **19**(21): p. 9399-411.

40. Halfter, W., et al., *The bi-functional organization of human basement membranes.* PLoS One, 2013. **8**(7): p. e67660.

41. Halfter, W., et al., *Temporary disruption of the retinal basal lamina and its effect on retinal histogenesis.* Dev Biol, 2001. **238**(1): p. 79-96.

42. Halfter, W., et al., *Origin and turnover of ECM proteins from the inner limiting membrane and vitreous body.* Eye (Lond), 2008. **22**(10): p. 1207-13.

43. Fletcher, E.L., et al., *Animal models of retinal disease.* Prog Mol Biol Transl Sci, 2011. **100**: p. 211-86.

44. Carr, A.J., et al., *Protective effects of human iPS-derived retinal pigment epithelium cell transplantation in the retinal dystrophic rat.* PLoS One, 2009. **4**(12): p. e8152.

45. Lu, B., et al., *Long-term safety and function of RPE from human embryonic stem cells in preclinical models of macular degeneration.* Stem Cells, 2009. **27**(9): p. 2126-35.

46. Lund, R.D., et al., *Human embryonic stem cell-derived cells rescue visual function in dystrophic RCS rats.* Cloning Stem Cells, 2006. **8**(3): p. 189-99.

47. Qu, Z., et al., *Transplantation of rat embryonic stem cell-derived retinal progenitor cells preserves the retinal structure and function in rat retinal degeneration.* Stem Cell Res Ther, 2015. **6**: p. 219.

48. Singh, R.K., et al., *Characterization of Three-Dimensional Retinal Tissue Derived from Human Embryonic Stem Cells in Adherent Monolayer Cultures.* Stem Cells Dev, 2015. **24**(23): p. 2778-95.

49. Schwartz, S.D., et al., *Embryonic stem cell trials for macular degeneration: a preliminary report.* Lancet, 2012. **379**(9817): p. 713-20.

50. Schwartz, S.D., et al., *Human embryonic stem cell-derived retinal pigment epithelium in patients with age-related macular degeneration and Stargardt's macular dystrophy: follow-up of two open-label phase 1/2 studies.* Lancet, 2015. **385**(9967): p. 509-16.

51. Mandai, M., Y. Kurimoto, and M. Takahashi, *Autologous Induced Stem-Cell-Derived Retinal Cells for Macular Degeneration.* N Engl J Med, 2017. **377**(8): p. 792-793.

52. De Schaepdrijver, L., et al., *Morphologic and clinical study of the retinal circulation in the miniature pig. B: Fluorescein angiography of the retina.* Exp Eye Res, 1992. **54**(6): p. 975-85.

53. Simoens, P., L. De Schaepdrijver, and H. Lauwers, *Morphologic and clinical study of the retinal circulation in the miniature pig. A: Morphology of the retinal microvasculature.* Exp Eye Res, 1992. **54**(6): p. 965-73.

54. Voss Kyhn, M., et al., *The multifocal electroretinogram (mfERG) in the pig.* Acta Ophthalmol Scand, 2007. **85**(4): p. 438-44.

55. Brant Fernandes, R.A., et al., *An Innovative Surgical Technique for Subretinal Transplantation of Human Embryonic Stem Cell-Derived Retinal Pigmented Epithelium in Yucatan Mini Pigs: Preliminary Results.* Ophthalmic Surg Lasers Imaging Retina, 2016. **47**(4): p. 342-51.

56. Sohn, E.H., et al., *Allogenic iPSC-derived RPE cell transplants induce immune response in pigs: a pilot study.* Sci Rep, 2015. **5**: p. 11791.

57. Zhou, L., et al., *Differentiation of induced pluripotent stem cells of swine into rod photoreceptors and their integration into the retina.* Stem Cells, 2011. **29**(6): p. 972-80.

58. Klassen, H., et al., *Photoreceptor Differentiation following Transplantation of Allogeneic Retinal Progenitor Cells to the Dystrophic Rhodopsin Pro347Leu Transgenic Pig.* Stem Cells Int, 2012. **2012**: p. 939801.

59. Warfvinge, K., et al., *Retinal progenitor cell xenografts to the pig retina: morphologic integration and cytochemical differentiation.* Arch Ophthalmol, 2005. **123**(10): p. 1385-93.

60. Libby, R.T., et al., *Laminin expression in adult and developing retinae: evidence of two novel CNS laminins.* J Neurosci, 2000. **20**(17): p. 6517-28.

61. Tetreault, N., M.P. Champagne, and G. Bernier, *The LIM homeobox transcription factor Lhx2 is required to specify the retina field and synergistically cooperates with Pax6 for Six6 trans-activation.* Dev Biol, 2009. **327**(2): p. 541-50.

62. de Melo, J., et al., *Lhx2 Is an Essential Factor for Retinal Gliogenesis and Notch Signaling.* J Neurosci, 2016. **36**(8): p. 2391-405.

63. Casarosa, S., et al., *Xrx1 controls proliferation and multipotency of retinal progenitors.* Mol Cell Neurosci, 2003. **22**(1): p. 25-36.

64. van Heyningen, V. and K.A. Williamson, *PAX6 in sensory development.* Hum Mol Genet, 2002. **11**(10): p. 1161-7.

65. Mao, C.A., et al., *Rewiring the retinal ganglion cell gene regulatory network: Neurod1 promotes retinal ganglion cell fate in the absence of Math5.* Development, 2008. **135**(20): p. 3379-88.

66. Liu, W., et al., *All Brn3 genes can promote retinal ganglion cell differentiation in the chick.* Development, 2000. **127**(15): p. 3237-47.

67. Bibb, L.C., et al., *Temporal and spatial expression patterns of the CRX transcription factor and its downstream targets. Critical differences during human and mouse eye development.* Hum Mol Genet, 2001. **10**(15): p. 1571-9.

68. Furukawa, T., E.M. Morrow, and C.L. Cepko, *Crx, a novel otx-like homeobox gene, shows photoreceptor-specific expression and regulates photoreceptor differentiation.* Cell, 1997. **91**(4): p. 531-41.

69. Nishida, A., et al., *Otx2 homeobox gene controls retinal photoreceptor cell fate and pineal gland development.* Nat Neurosci, 2003. **6**(12): p. 1255-63.

70.   Burmeister, M., et al., *Ocular retardation mouse caused by Chx10 homeobox null allele: impaired retinal progenitor proliferation and bipolar cell differentiation.* Nat Genet, 1996. **12**(4): p. 376-84.

71.   Dorval, K.M., et al., *CHX10 targets a subset of photoreceptor genes.* J Biol Chem, 2006. **281**(2): p. 744-51.

72.   Ekstrom, P. and K. Johansson, *Differentiation of ganglion cells and amacrine cells in the rat retina: correlation with expression of HuC/D and GAP-43 proteins.* Brain Res Dev Brain Res, 2003. **145**(1): p. 1-8.

73.   Gill, K.P., et al., *Enriched retinal ganglion cells derived from human embryonic stem cells.* Sci Rep, 2016. **6**: p. 30552.

74.   Gnanaguru, G., et al., *Laminins containing the beta2 and gamma3 chains regulate astrocyte migration and angiogenesis in the retina.* Development, 2013. **140**(9): p. 2050-60.

75.   Varshney, S., D.D. Hunter, and W.J. Brunken, *Extracellular Matrix Components Regulate Cellular Polarity and Tissue Structure in the Developing and Mature Retina.* J Ophthalmic Vis Res, 2015. **10**(3): p. 329-39.

76.   Chang, B., et al., *Retinal degeneration mutants in the mouse.* Vision Res, 2002. **42**(4): p. 517-25.

77.   Gargini, C., et al., *Retinal organization in the retinal degeneration 10 (rd10) mutant mouse: a morphological and ERG study.* J Comp Neurol, 2007. **500**(2): p. 222-38.

78.   Gerth, C., et al., *Cone-mediated multifocal electroretinogram in age-related macular degeneration: progression over a long-term follow-up.* Arch Ophthalmol, 2006. **124**(3): p. 345-52.

79.   Kennelly, K.P., et al., *Early Subretinal Allograft Rejection Is Characterized by Innate Immune Activity.* Cell Transplant, 2017. **26**(6): p. 983-1000.

80.   Sugita, S., et al., *Successful Transplantation of Retinal Pigment Epithelial Cells from MHC Homozygote iPSCs in MHC-Matched Models.* Stem Cell Reports, 2016. **7**(4): p. 635-648.

81.   Qu, L., et al., *Combined transplantation of human mesenchymal stem cells and human retinal progenitor cells into the subretinal space of RCS rats.* Sci Rep, 2017. **7**(1): p. 199.

82.   Kundu, J., et al., *Decellularized retinal matrix: Natural platforms for human retinal progenitor cell culture.* Acta Biomater, 2016. **31**: p. 61-70.

83.   Miyazaki, T., et al., *Recombinant human laminin isoforms can support the undifferentiated growth of human embryonic stem cells.* Biochem Biophys Res Commun, 2008. **375**(1): p. 27-32.

84.   Rodin, S., et al., *Clonal culturing of human embryonic stem cells on laminin-521/E-cadherin matrix in defined and xeno-free environment.* Nat Commun, 2014. **5**: p. 3195.

85.   Fariss, R.N., Z.Y. Li, and A.H. Milam, *Abnormalities in rod photoreceptors, amacrine cells, and horizontal cells in human retinas with retinitis pigmentosa.* Am J Ophthalmol, 2000. **129**(2): p. 215-23.

86.   Jones, B.W., et al., *Retinal remodeling in the Tg P347L rabbit, a large-eye model of retinal degeneration.* J Comp Neurol, 2011. **519**(14): p. 2713-33.

87. Gonzalez-Cordero, A., et al., *Photoreceptor precursors derived from three-dimensional embryonic stem cell cultures integrate and mature within adult degenerate retina.* Nat Biotechnol, 2013. **31**(8): p. 741-7.

88. Koulen, P., et al., *Immunocytochemical localization of the postsynaptic density protein PSD-95 in the mammalian retina.* J Neurosci, 1998. **18**(23): p. 10136-49.

89. Dutescu, R.M., et al., *Multifocal ERG recordings under visual control of the stimulated fundus in mice.* Invest Ophthalmol Vis Sci, 2013. **54**(4): p. 2582-9.

90. Li, S.Y., et al., *Rescue from light-induced retinal degeneration by human fetal retinal transplantation in minipigs.* Curr Eye Res, 2009. **34**(7): p. 523-35.

91. Sorensen, N.B., et al., *Time-Dependent Decline in Multifocal Electroretinogram Requires Faster Recording Procedures in Anesthetized Pigs.* Transl Vis Sci Technol, 2017. **6**(2): p. 6.

92. Rizzolo, L.J., *Basement membrane stimulates the polarized distribution of integrins but not the Na,K-ATPase in the retinal pigment epithelium.* Cell Regul, 1991. **2**(11): p. 939-49.

93. Lynn, S.A., et al., *Ex-vivo models of the Retinal Pigment Epithelium (RPE) in long-term culture faithfully recapitulate key structural and physiological features of native RPE.* Tissue Cell, 2017. **49**(4): p. 447-460.

94. McLenachan, S., et al., *Bioengineered Bruch's-like extracellular matrix promotes retinal pigment epithelial differentiation.* Biochem Biophys Rep, 2017. **10**: p. 178-185.

95. Xiang, P., et al., *A novel Bruch's membrane-mimetic electrospun substrate scaffold for human retinal pigment epithelium cells.* Biomaterials, 2014. **35**(37): p. 9777-9788.